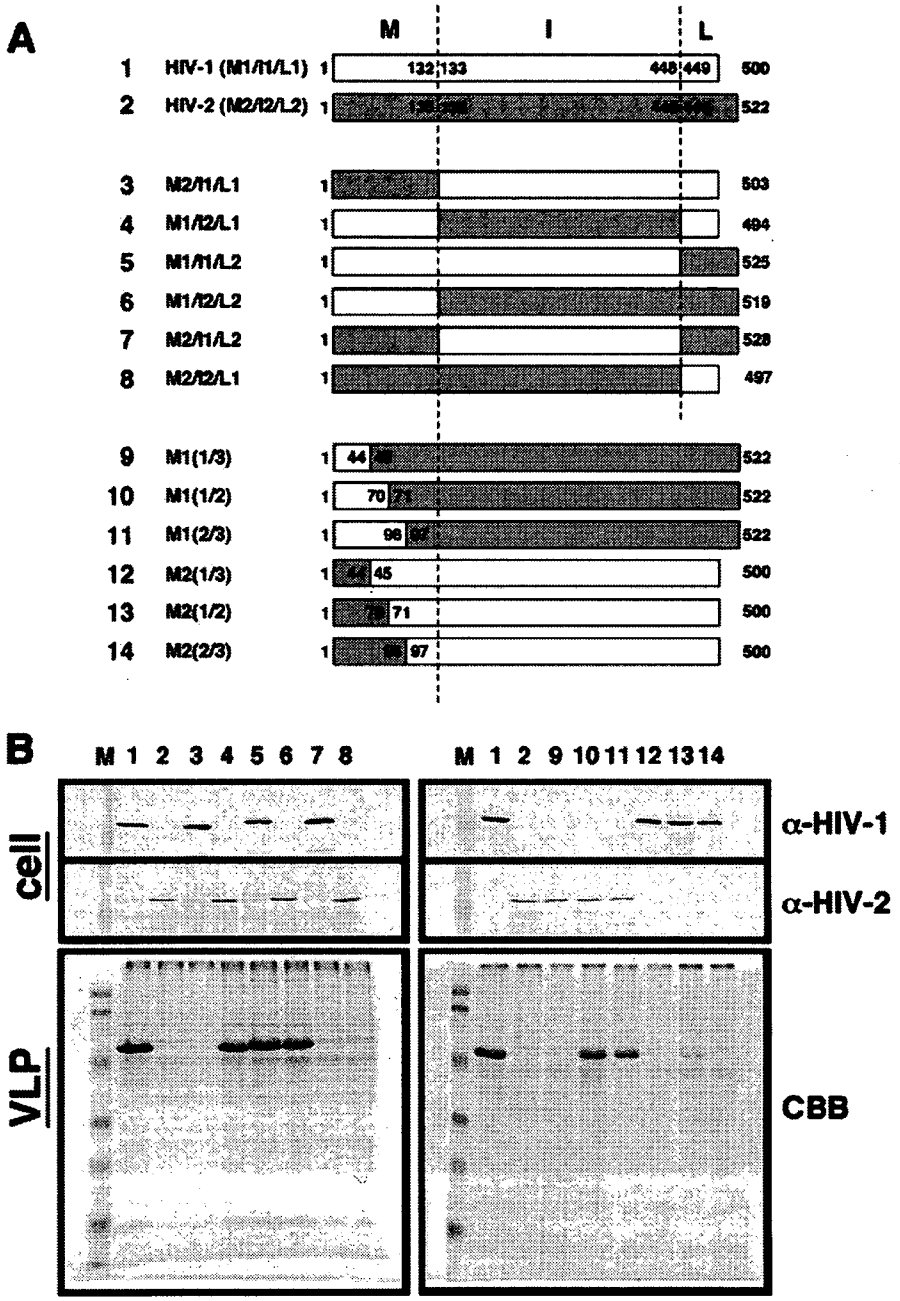

FIG. 7. Mapping of HIV-2 Gag regions inhibitory for Gag VLP production in yeast. (A) Schematic representation of chimeric Gags constructed between HIV-1 and HIV-2. (B) Intracellular Gag expression and Gag VLP production. Yeast cells were transformed with a pKT10 vector containing each Gag construct. Intracellular Gag expression was analyzed by Western blotting using anti-HIV-1 CA and anti-HIV-2 CA antibodies. Production and purification of Gag VLPs were carried out as described in the legend for Fig. 1. Gag VLPs were analyzed by SDS-PAGE followed by CBB staining. Lanes: M, prestained molecular weight markers; 1 and 2, expression of HIV-1 and HIV-2 Gag, respectively; 3 to 14, expression of chimeric Gags M2/I1/L1, M1/I2/L1, M1/I1/L2, M1/I2/L2, M2/I1/L2, M2/I2/L1, M1(1/3), M1(1/2), M1(2/3), M2(1/3), M2(1/2), and M2(2/3), respectively.

located near the end of helix 2 of MA, into HIV-1 Gag [construct 1(ANK)] (Fig. 8B). Introduction of the corresponding sequence of HIV-1 into HIV-2, however, did not confer particle production, although this was expected from the fact that the M1(1/3) construct did not produce Gag VLP (Fig. 7). We prepared the whole-cell lysates from several of the substitution mutants and examined their ability to form high-order Gag multimers by sedimentation analysis. The VLP-competent Gag mutants showed both high- and low-order Gag multimers, while in contrast, the VLP-incompetent Gag mutants showed only the low-order form (Fig. 8C). The 1(ANK) Gag construct did not show membrane affinity when samples were prepared in the absence of salt and subjected to membrane flotation analysis (Fig. 8D). These data indicate that a defined region of HIV-2 MA may affect stable

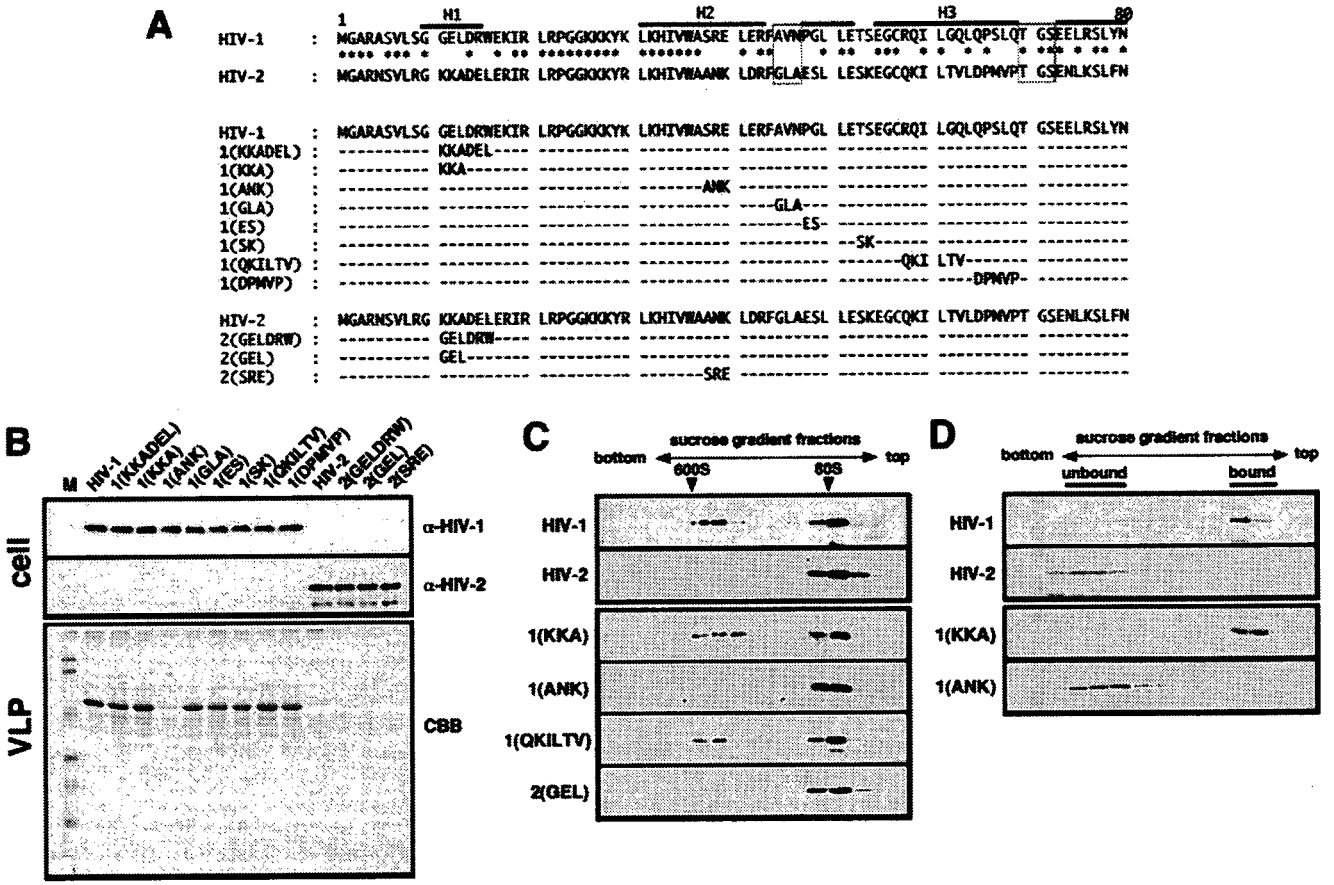

FIG. 8. Defining the N-terminal HIV-2 MA region inhibitory for Gag assembly and VLP production in yeast. (A) Amino acid alignment of Gag mutants with amino acid substitutions. The trimerization sites are shown in boxes, and helices 1 to 3 are shown as H1 to H3. (B) Intracellular expression and VLP production of Gag mutants. Protein expression and Gag VLP production in yeast were carried out as described in the legend for Fig. 1. Cell samples were subjected to Western blotting using anti-HIV-1 CA and anti-HIV-2 CA antibodies, and Gag VLPs were analyzed by SDS-PAGE followed by CBB staining. Lane M shows prestained molecular weight markers. (C) Sedimentation analysis of Gag mutants. Protein expression in yeast was carried out as described in the legend for Fig. 3. The whole-cell lysate was subjected to sedimentation analysis with a 20 to 70% sucrose gradient by centrifugation at 120,000 × *g* for 2 h, and gradient fractions were subjected to Western blotting using anti-Flag antibody. Arrowheads show sedimented positions of the immature form of HIV capsid (60OS) and of 80S ribosomes. (D) Membrane affinities of Gag mutants in the absence of salt. Protein expression in yeast was carried out as described in the legend for Fig. 3, and equilibrium flotation centrifugation was described in the legend for Fig. 4. Gradient fractions were analyzed by Western blotting using anti-Flag antibody.

membrane affinity and high-order Gag assembly and, as a result, lead to the failure of VLP production in yeast.

DISCUSSION

The Gag proteins of primate lentiviral lineages have approximately 55 to 60% amino acid sequence identity between each of the lineages (8). In this study, we used Gag proteins of four different primate lentiviral lineages and analyzed their ability to produce Gag VLPs in yeast. We found that the Gag protein of the HIV-2/SIVmac lineage failed to release Gag VLPs in yeast, despite the fact that the Gag protein was myristoylated and targeted to the plasma membrane. The failure of HIV-2 Gag VLP production was likely due to the lack of high-order Gag multimerization but was also accompanied by an unstable association of Gag with the membrane. These findings were not observed in higher eukaryotic cells, suggesting that a host factor(s) was involved.

A host factor involved in Gag multimerization, ABCE1/HP68, has been identified by in vitro translation studies showing that this factor associates with relatively high-order Gag multimers but not with a lower-order form and facilitates Gag assembly into a VLP form as a molecular chaperone (56). Immunodepletion of ABCE1/HP68 in the in vitro reactions reduced the higher-order form with the accumulation of lower-order forms (56), a condition which was ostensibly similar to the failure of HIV-2 Gag assembly in yeast. However, this host factor is highly conserved in eukaryotes, including yeast, and has been shown to support all primate lentiviral Gag assembly (10). Later studies have shown that the NC but not MA domain is critical for Gag-ABCE1/HP68 interaction (23). From these data, it is unlikely that the putative host factor suggested in this study is ABCE1/HP68.

Primate lentiviral MA is composed of five helices, with helices 1 and 2 located on the upper surface of a globular MA structure in which the N-terminal basic residues are clustered.

In the MA trimer model, the myristoyl moiety and N-terminal basic residues act in synergy to stabilize the trimer on an acidic membrane (18). Recent studies have further indicated that $PI(4,5)P_2$, a lipid involved in membrane targeting of Gag (31), binds to a hydrophobic cleft formed with highly conserved amino acids by helices 2 and 4 and contributes to the membrane affinity of MA (41). Our data showed that the dominant region responsible for the failure of HIV-2 Gag VLP production was mapped near the end of helix 2 of MA, a site distinct from the MA trimerization site or the $PI(4,5)P_2$ binding cleft. The blockage of HIV-2 Gag VLP production in yeast occurred at the process of particle budding rather than Gag transport, and the membrane affinity of Gag was weakened. These facts suggest that such a host factor would be a component(s) including certain lipids present on or recruited to the plasma membrane, but the lipids would not be $PI(4,5)P_2$, and indeed, $PI(4,5)P_2$ is widely present in eukaryotes, including yeast. These data raise the alternative possibility that yeast may have an inhibitory factor(s) for HIV-2 Gag assembly.

Although it has been accepted that Gag oligomerization and membrane targeting are essentially independent events, recent studies have suggested that the membrane affinity of Gag may be promoted by Gag multimerization (43, 55). Another study indicated that the N-terminal myristoyl moiety of MA was exposed when MA formed a trimer (49). However, it is also possible that unstable membrane binding of Gag may not facilitate Gag multimerization, resulting in a lack of high-order assembly. In this study, we observed that the defects in Gag multimerization and membrane affinity occurred concomitantly in yeast, but we cannot prove, at present, which directly affected the failure of HIV-2 Gag VLP production in our system. In favor of the former possibility, the lack of a high-order Gag multimer was observed even at a physiological concentration of salt, a condition under which HIV-2 Gag associated with the yeast membrane. In contrast, the latter possibility would be supported by the data that (i) the region we mapped was located at helix 2 of MA, facing the membrane; (ii) in the MA trimer model (18, 38), this region is located near the center of the trimer, suggesting little possibility of involvement in higher-order Gag assembly; and (iii) the introduction of only three amino acids of HIV-2 Gag (located at the region) into the HIV-1 background, in which Gag multimerization domains are intact, failed to produce Gag VLPs.

The membrane affinity of Gag is regulated by N-myristoylation but also by the basic amino acid clusters in the M domain (4, 14, 15, 35, 54). In our study, the failure of HIV-2 Gag VLP production was accompanied by the dissociation of Gag from the membrane, a phenomenon which was observed only in the absence of salt. In general, relatively high concentrations of salt, such as 500 mM NaCl, disrupt electrostatic protein bonds but do not affect hydrophobic bonds. Conversely, in the absence of salt, hydrophobic but not electrostatic interactions are often disrupted. We observed that neither HIV-1 nor HIV-2 Gag dissociated from the membrane in the presence of 500 mM NaCl, suggesting that the N-terminal myristoyl moiety is a dominant determinant for membrane binding of Gag in yeast and that the membrane affinities of Gag mediated by the myristoyl moiety were comparable between the two Gags. In contrast, HIV-2 Gag dissociated from the yeast membrane in the absence of salt, under which condition HIV-1 Gag remained associated. These results suggest that the electrostatic interactions of HIV-2 Gag with the yeast membrane were weaker than those of HIV-1 Gag, leading to Gag dissociation from the yeast membrane. The amino acid sequences of the MA helix 2 region we mapped for the four primate lentiviral lineages are as follows: HIV-1, SRE; HIV-2, ANK; SIVmac, ANE; SIVagm, GKE; and SIVmnd, KGE.

Mutational studies of the N-terminal region of MA have suggested the involvement of hydrophobicity and electrostatic interactions of MA in Gag relocation and membrane extrusion. Amino acid substitutions in the MA basic domain redirected Gag to the endoplasmic reticulum and endosomes (34, 35, 54). Mutations of hydrophobic residues near the N terminus of MA to less hydrophobic residues severely impaired membrane binding of Gag without inhibiting N-terminal myristoylation, suggesting a failure of membrane insertion of the myristoyl moiety (36). Interestingly, in Mason-Pfizer monkey virus, a prototype for capsid formation prior to membrane relocation, an increase in the hydrophobicity of MA led to arrest at an early stage of particle budding, possibly by inhibiting exposure of the N-terminal myristoyl moiety (45). Thus, it cannot be ruled out that in our study, the absence of salt may have caused a disruption of the gross conformation of Gag (e.g., unfolding of the hydrophobic core of MA) and/or led to sequestration of the N-terminal myristoyl moiety.

ACKNOWLEDGMENTS

We thank S. Morikawa (National Institute of Infectious Diseases, Japan) for supply of the *gag* gene of SIVagm and the anti-SIVagm monkey serum and T. Miura (Kyoto University, Japan) for supply of the *gag* gene of SIVmnd. The cDNA of HIV-2 (ROD strain) was provided by the NIH AIDS Research and Reference Reagent Program. We also thank K. Mizumoto (Kitasato University, Japan) for supply of a yeast expression vector.

This work was supported by an AIDS grant from the Ministry of Health, Labor, and Welfare of Japan and by a grant-in-aid for scientific research from the Japan Society for the Promotion of Science.

REFERENCES

1. **Bagnat, M., S. Keranen, A. Shevchenko, and K. Simons.** 2000. Lipid rafts function in biosynthetic delivery of proteins to the cell surface in yeast. Proc. Natl. Acad. Sci. USA **97**:3254–3259.
2. **Bieniasz, P. D.** 2003. Restriction factors: a defense against retroviral infection. Trends Microbiol. **11**:286–291.
3. **Braaten, D., and J. Luban.** 2001. Cyclophilin A regulates HIV-1 infectivity, as demonstrated by gene targeting in human T cells. EMBO J. **20**:1300–1309.
4. **Bryant, M., and L. Ratner.** 1990. Myristoylation-dependent replication and assembly of human immunodeficiency virus 1. Proc. Natl. Acad. Sci. USA **87**:523–527.
5. **Campbell, S., and A. Rein.** 1999. In vitro assembly properties of human immunodeficiency virus type 1 Gag protein lacking the p6 domain. J. Virol. **73**:2270–2279.
6. **Campbell, S., and V. M. Vogt.** 1997. In vitro assembly of virus-like particles with Rous sarcoma virus Gag deletion mutants: identification of the p10 domain as a morphological determinant in the formation of spherical particles. J. Virol. **71**:4425–4435.
7. **Carriere, C., B. Gay, N. Chazal, N. Morin, and P. Boulanger.** 1995. Sequence requirements for encapsidation of deletion mutants and chimeras of human immunodeficiency virus type 1 Gag precursor into retrovirus-like particles. J. Virol. **69**:2366–2377.
8. **Desrosiers, R. C.** 1990. HIV-1 origins. A finger on the missing link. Nature **345**:288–289.
9. **Dong, X., H. Li, A. Derdowski, L. Ding, A. Burnett, X. Chen, T. R. Peters, T. S. Dermody, E. Woodruff, J. J. Wang, and P. Spearman.** 2005. AP-3 directs the intracellular trafficking of HIV-1 Gag and plays a key role in particle assembly. Cell **120**:663–674.
10. **Dooher, J. E., and J. R. Lingappa.** 2004. Conservation of a stepwise, energy-sensitive pathway involving HP68 for assembly of primate lentivirus capsids in cells. J. Virol. **78**:1645–1656.
11. **Dorfman, T., A. Bukovsky, A. Ohagen, S. Hoglund, and H. G. Gottlinger.**

1994. Functional domains of the capsid protein of human immunodeficiency virus type 1. J. Virol. **68**:8180–8187.
12. **Garrus, J. E., U. K. von Schwedler, O. W. Pornillos, S. G. Morham, K. H. Zavitz, H. E. Wang, D. A. Wettstein, K. M. Stray, M. Cote, R. L. Rich, D. G. Myszka, and W. I. Sundquist.** 2001. Tsg101 and the vacuolar protein sorting pathway are essential for HIV-1 budding. Cell **107**:55–65.
13. **Gerrard, S. R., B. P. Levi, and T. H. Stevens.** 2000. Pep12p is a multifunctional yeast syntaxin that controls entry of biosynthetic, endocytic and retrograde traffic into the prevacuolar compartment. Traffic **1**:259–269.
14. **Gheysen, D., E. Jacobs, F. de Foresta, C. Thiriart, M. Francotte, D. Thines, and M. De Wilde.** 1989. Assembly and release of HIV-1 precursor Pr55^{gag} virus-like particles from recombinant baculovirus-infected insect cells. Cell **59**:103–112.
15. **Gottlinger, H. G., J. G. Sodroski, and W. A. Haseltine.** 1989. Role of capsid precursor processing and myristoylation in morphogenesis and infectivity of human immunodeficiency virus type 1. Proc. Natl. Acad. Sci. USA **86**:5781–5785.
16. **Gottlinger, H. G., T. Dorfman, J. G. Sodroski, and W. A. Haseltine.** 1991. Effect of mutations affecting the p6 gag protein on human immunodeficiency virus particle release. Proc. Natl. Acad. Sci. USA **88**:3195–3199.
17. **Hahn, B. H., G. M. Shaw, K. M. De Cock, and P. M. Sharp.** 2000. AIDS as a zoonosis: scientific and public health implications. Science **287**:607–614.
18. **Hill, C. P., D. Worthylake, D. P. Bancroft, A. M. Christensen, and W. I. Sundquist.** 1996. Crystal structures of the trimeric human immunodeficiency virus type 1 matrix protein: implications for membrane association and assembly. Proc. Natl. Acad. Sci. USA **93**:3099–3104.
19. **Hoshikawa, N., A. Kojima, A. Yasuda, E. Takayashiki, S. Masuko, J. Chiba, T. Sata, and T. Kurata.** 1991. Role of the *gag* and *pol* genes of human immunodeficiency virus in the morphogenesis and maturation of retrovirus-like particles expressed by recombinant vaccinia virus: an ultrastructural study. J. Gen. Virol. **72**:2509–2517.
20. **Keckesova, Z., L. M. Ylinen, and G. J. Towers.** 2004. The human and African green monkey TRIM5alpha genes encode Ref1 and Lv1 retroviral restriction factor activities. Proc. Natl. Acad. Sci. USA **101**:10780–10785.
21. **Kikonyogo, A., F. Bouamr, M. L. Vana, Y. Xiang, A. Aiyar, C. Carter, and J. Leis.** 2001. Proteins related to the Nedd4 family of ubiquitin protein ligases interact with the L domain of Rous sarcoma virus and are required for gag budding from cells. Proc. Natl. Acad. Sci. USA **98**:11199–11204.
22. **Klikova, M., S. S. Rhee, E. Hunter, and T. Ruml.** 1995. Efficient in vivo and in vitro assembly of retroviral capsids from Gag precursor proteins expressed in bacteria. J. Virol. **69**:1093–1098.
23. **Lingappa, J. R., J. E. Dooher, M. A. Newman, P. K. Kiser, and K. C. Klein.** 2006. Basic residues in the nucleocapsid domain of Gag are required for interaction of HIV-1 Gag with ABCE1 (HP68), a cellular protein important for HIV-1 capsid assembly. J. Biol. Chem. **281**:3773–3784.
24. **Mammano, F., A. Ohagen, S. Hoglund, and H. G. Gottlinger.** 1994. Role of the major homology region of human immunodeficiency virus type 1 in virion morphogenesis. J. Virol. **68**:4927–4936.
25. **Massiah, M. A., M. R. Starich, C. Paschall, M. F. Summers, A. M. Christensen, and W. I. Sundquist.** 1994. Three-dimensional structure of the human immunodeficiency virus type 1 matrix protein. J. Mol. Biol. **244**:198–223.
26. **Matthews, S., P. Barlow, J. Boyd, G. Barton, R. Russell, H. Mills, M. Cunningham, N. Meyers, N. Burns, N. Clark, S. Kingsman, A. Kingsman, and I. Campbell.** 1994. Structural similarity between the p17 matrix protein of HIV-1 and interferon-gamma. Nature **370**:666–668.
27. **Morikawa, Y., T. Goto, and K. Sano.** 1999. *In vitro* assembly of human immunodeficiency virus type 1 Gag protein. J. Biol. Chem. **274**:27997–28002.
28. **Morikawa, Y., T. Goto, and F. Momose.** 2004. Human immunodeficiency virus type 1 Gag assembly through assembly intermediates. J. Biol. Chem. **279**:31964–31972.
29. **Nguyen, D. H., and J. E. Hildreth.** 2000. Evidence for budding of human immunodeficiency virus type 1 selectively from glycolipid-enriched membrane lipid rafts. J. Virol. **74**:3264–3272.
30. **Niwa, H., K. Yamamura, and J. Miyazaki.** 1991. Efficient selection for high-expression transfectants with a novel eukaryotic vector. Gene **108**:193–199.
31. **Ono, A., S. D. Ablan, S. J. Lockett, K. Nagashima, and E. O. Freed.** 2004. Phosphatidylinositol (4,5) bisphosphate regulates HIV-1 Gag targeting to the plasma membrane. Proc. Natl. Acad. Sci. USA **101**:14889–14894.
32. **Ono, A., and E. O. Freed.** 1999. Binding of human immunodeficiency virus type 1 Gag to membrane: role of the matrix amino terminus. J. Virol. **73**:4136–4144.
33. **Ono, A., and E. O. Freed.** 2001. Plasma membrane rafts play a critical role in HIV-1 assembly and release. Proc. Natl. Acad. Sci. USA **98**:13925–13930.
34. **Ono, A., and E. O. Freed.** 2004. Cell-type-dependent targeting of human immunodeficiency virus type 1 assembly to the plasma membrane and the multivesicular body. J. Virol. **78**:1552–1563.
35. **Ono, A., J. M. Orenstein, and E. O. Freed.** 2000. Role of the Gag matrix domain in targeting human immunodeficiency virus type 1 assembly. J. Virol. **74**:2855–2866.
36. **Paillart, J. C., and H. G. Gottlinger.** 1999. Opposing effects of human immunodeficiency virus type 1 matrix mutations support a myristyl switch model of Gag membrane targeting. J. Virol. **73**:2604–2612.
37. **Parent, L. J., R. P. Bennett, R. C. Craven, T. D. Nelle, N. K. Krishna, J. B. Bowzard, C. B. Wilson, B. A. Puffer, R. C. Montelaro, and J. W. Wills.** 1995. Positionally independent and exchangeable late budding functions of the Rous sarcoma virus and human immunodeficiency virus Gag proteins. J. Virol. **69**:5455–5460.
38. **Rao, Z., A. S. Belyaev, E. Fry, P. Roy, I. M. Jones, and D. I. Stuart.** 1995. Crystal structure of SIV matrix antigen and implications for virus assembly. Nature **378**:743–747.
39. **Reicin, A. S., S. Paik, R. D. Berkowitz, J. Luban, I. Lowy, and S. P. Goff.** 1995. Linker insertion mutations in the human immunodeficiency virus type 1 *gag* gene: effects on virion particle assembly, release, and infectivity. J. Virol. **69**:642–650.
40. **Ruggieri, R., K. Tanaka, M. Nakafuku, Y. Kaziro, A. Toh-e, and K. Matsumoto.** 1989. *MSI1*, a negative regulator of the RAS-cAMP pathway in *Saccharomyces cerevisiae*. Proc. Natl. Acad. Sci. USA **86**:8778–8782.
41. **Saad, J. S., J. Miller, J. Tai, A. Kim, R. H. Ghanam, and M. F. Summers.** 2006. Structural basis for targeting HIV-1 Gag proteins to the plasma membrane for virus assembly. Proc. Natl. Acad. Sci. USA **103**:11364–11369.
42. **Sakuragi, S., T. Goto, K. Sano, and Y. Morikawa.** 2002. HIV type 1 Gag virus-like particle budding from spheroplasts of *Saccharomyces cerevisiae*. Proc. Natl. Acad. Sci. USA **99**:7956–7961.
43. **Sandefur, S., V. Varthakavi, and P. Spearman.** 1998. The I domain is required for efficient plasma membrane binding of human immunodeficiency virus type 1 Pr55Gag. J. Virol. **72**:2723–2732.
44. **Smith, A. J., N. Srinivasakumar, M. L. Hammarskjold, and D. Rekosh.** 1993. Requirements for incorporation of Pr160$^{gag\text{-}pol}$ from human immunodeficiency virus type 1 into virus-like particles. J. Virol. **67**:2266–2275.
45. **Stansell, E., E. Tytler, M. R. Walter, and E. Hunter.** 2004. An early stage of Mason-Pfizer monkey virus budding is regulated by the hydrophobicity of the Gag matrix domain core. J. Virol. **78**:5023–5031.
46. **Strack, B., A. Calistri, S. Craig, E. Popova, and H. G. Gottlinger.** 2003. AIP1/ALIX is a binding partner for HIV-1 p6 and EIAV p9 functioning in virus budding. Cell **114**:689–699.
47. **Stremlau, M., C. M. Owens, M. J. Perron, M. Kiessling, P. Autissier, and J. Sodroski.** 2004. The cytoplasmic body component TRIM5alpha restricts HIV-1 infection in Old World monkeys. Nature **427**:848–853.
48. **Tanaka, K., M. Nakafuku, F. Tamanoi, Y. Kaziro, K. Matsumoto, and A. Toh-e.** 1990. *IRA2*, a second gene of *Saccharomyces cerevisiae* that encodes a protein with a domain homologous to mammalian *ras* GTPase-activating protein. Mol. Cell. Biol. **10**:4303–4313.
49. **Tang, C., E. Loeliger, P. Luncsford, I. Kinde, D. Beckett, and M. F. Summers.** 2004. Entropic switch regulates myristate exposure in the HIV-1 matrix protein. Proc. Natl. Acad. Sci. USA **101**:517–522.
50. **Towers, G. J., T. Hatziioannou, S. Cowan, S. P. Goff, J. Luban, and P. D. Bieniasz.** 2003. Cyclophilin A modulates the sensitivity of HIV-1 to host restriction factors. Nat. Med. **9**:1138–1143.
51. **Towler, D. A., S. P. Adams, S. R. Eubanks, D. S. Towery, E. Jackson-Machelski, L. Glaser, and J. I. Gordon.** 1988. Myristoyl CoA: protein N-myristoyltransferase activities from rat liver and yeast possess overlapping yet distinct peptide substrate specificities. J. Biol. Chem. **263**:1784–1790.
52. **VerPlank, L., F. Bouamr, T. J. LaGrassa, B. Agresta, A. Kikonyogo, J. Leis, and C. A. Carter.** 2001. Tsg101, a homologue of ubiquitin-conjugating (E2) enzymes, binds the L domain in HIV type 1 Pr55(Gag). Proc. Natl. Acad. Sci. USA **98**:7724–7729.
53. **von Schwedler, U. K., M. Stuchell, B. Muller, D. M. Ward, H. Y. Chung, E. Morita, H. E. Wang, T. Davis, G. P. He, D. M. Cimbora, A. Scott, H. G. Krausslich, J. Kaplan, S. G. Morham, and W. I. Sundquist.** 2003. The protein network of HIV budding. Cell **114**:701–713.
54. **Yuan, X., X. Yu, T. H. Lee, and M. Essex.** 1993. Mutations in the N-terminal region of human immunodeficiency virus type 1 matrix protein block intracellular transport of the Gag precursor. J. Virol. **67**:6387–6394.
55. **Zhou, W., and M. D. Resh.** 1996. Differential membrane binding of the human immunodeficiency virus type 1 matrix protein. J. Virol. **70**:8540–8548.
56. **Zimmerman, C., K. C. Klein, P. K. Kiser, A. R. Singh, B. L. Firestein, S. C. Riba, and J. R. Lingappa.** 2002. Identification of a host protein essential for assembly of immature HIV-1 capsids. Nature **415**:88–92.

JOURNAL OF VIROLOGY, Nov. 2007, p. 11640–11649 Vol. 81, No. 21
0022-538X/07/$08.00+0 doi:10.1128/JVI.01475-07

Induction of CD8$^+$ Cells Able To Suppress CCR5-Tropic Simian Immunodeficiency Virus SIVmac239 Replication by Controlled Infection of CXCR4-Tropic Simian-Human Immunodeficiency Virus in Vaccinated Rhesus Macaques$^\nabla$

Tetsuo Tsukamoto,[1,2]† Mitsuhiro Yuasa,[1]† Hiroyuki Yamamoto,[1] Miki Kawada,[1,2] Akiko Takeda,[1] Hiroko Igarashi,[2] and Tetsuro Matano[1,2,3,4]*

International Research Center for Infectious Diseases, The Institute of Medical Science, The University of Tokyo, 4-6-1 Shirokanedai, Minato-Ku, Tokyo 108-8639, Japan[1]; Graduate School of Medicine, The University of Tokyo, 7-3-1 Hongo, Bunkyo-Ku, Tokyo 113-0033, Japan[2]; AIDS Research Center, National Institute of Infectious Diseases, 1-23-1 Toyama, Shinjuku-ku, Tokyo 162-8640, Japan[3]; and Tsukuba Primate Research Center, National Institute of Biomedical Innovation, 1 Hachimandai, Tsukuba, Ibaraki 305-0843, Japan[4]

Received 5 July 2007/Accepted 16 August 2007

Recent recombinant viral vector-based AIDS vaccine trials inducing cellular immune responses have shown control of CXCR4-tropic simian-human immunodeficiency virus (SHIV) replication but difficulty in containment of pathogenic CCR5-tropic simian immunodeficiency virus (SIV) in rhesus macaques. In contrast, controlled infection of live attenuated SIV/SHIV can confer the ability to contain SIV superchallenge in macaques. The specific immune responses responsible for this control may be induced by live virus infection but not consistently by viral vector vaccination, although those responses have not been determined. Here, we have examined in vitro anti-SIV efficacy of CD8$^+$ cells in rhesus macaques that showed prophylactic viral vector vaccine-based control of CXCR4-tropic SHIV89.6PD replication. Analysis of the effect of CD8$^+$ cells obtained at several time points from these macaques on CCR5-tropic SIVmac239 replication in vitro revealed that CD8$^+$ cells in the chronic phase after SHIV challenge suppressed SIV replication more efficiently than those before challenge. SIVmac239 superchallenge of two of these macaques at 3 or 4 years post-SHIV challenge was contained, and the following anti-CD8 antibody administration resulted in transient CD8$^+$ T-cell depletion and appearance of plasma SIVmac239 viremia in both of them. Our results indicate that CD8$^+$ cells acquired the ability to efficiently suppress SIV replication by controlled SHIV infection, suggesting the contribution of CD8$^+$ cell responses induced by controlled live virus infection to containment of HIV/SIV superinfection.

Live attenuated immunodeficiency virus infection can induce effective immune responses against pathogenic human immunodeficiency virus type 1 (HIV-1) and simian immunodeficiency virus (SIV) replication, although concerns about conditions necessary for its safety as an AIDS vaccine have not been satisfied at present (3, 13, 19). In macaque AIDS models, infection of live attenuated viruses such as SIVmac239Δnef, SIVmac239Δ3, and simian-human immunodeficiency virus (SHIV) 89.6 have been shown to confer potent immune responses resulting in control of SIV superchallenge (7, 14, 35, 53). While involvement of virus-specific CD8$^+$ cytotoxic T-lymphocyte (CTL) responses has been indicated, it has remained unclear what immune responses play a key role in this control (19, 34).

Virus-specific cellular immune responses are crucial for control of HIV-1 and SIV infections (1, 4, 5, 10, 12, 20, 29, 38, 41, 42). Recombinant viral vector-based vaccines efficiently eliciting virus-specific cellular immune responses have been developed as promising AIDS vaccine candidates (32). These prophylactic vaccine trials in rhesus macaques have shown viral control and prevention of acute CD4$^+$ T-cell depletion after CXCR4-tropic SHIV challenge (2, 27, 36, 37, 40, 46). Unfortunately, however, trials of these vaccines have shown difficulty in containment of CCR5-tropic SIV infection that induces acute, massive depletion of CCR5$^+$ CD4$^+$ memory T cells and chronic disease progression like HIV-1 infection in humans (6, 8, 11, 21, 23, 28, 30, 31, 39, 49, 50, 52). Possibly, the specific immune responses responsible for SIV control might be induced by live SIV/SHIV infection but not consistently by recombinant viral vector vaccination. Previous CD8$^+$ cell-depletion experiments in macaques using a monoclonal anti-CD8 antibody have indicated the importance of CD8$^+$ cells in SIV control (12, 29, 42), but differences in antiviral efficacy between live SIV/SHIV infection-induced and recombinant viral vector vaccination-induced CD8$^+$ cells have not been determined.

Our previous trials of a prophylactic vaccine using a Gag-expressing Sendai virus (SeV-Gag) vector have shown control of CXCR4-tropic SHIV89.6PD replication in vaccinated rhesus macaques (27, 47). While this vaccination did not always result in CCR5-tropic SIVmac239 control (28), it was speculated that, after SHIV challenge, these vaccinees may possibly

* Corresponding author. Mailing address: International Research Center for Infectious Diseases, The Institute of Medical Science, The University of Tokyo, 4-6-1 Shirokanedai, Minato-ku, Tokyo 108-8639, Japan. Phone: 81-3-6409-2078. Fax: 81-3-6409-2076. E-mail: matano@m.u-tokyo.ac.jp.

† T.T. and M.Y. contributed equally to this work.

$^\nabla$ Published ahead of print on 29 August 2007.

TABLE 1. Virus challenge and antibody administration schedule

Macaque	Prophylactic vaccination	Time (wk) of:			
		SHIV89.6PD challenge	Anti-CD20 monoclonal antibody administration	SIVmac239 superchallenge	Anti-CD8 monoclonal antibody administration
R00-017	SeV-Gag	0	166	203	209
R00-020	DNA prime with SeV-Gag boost	0	140	151	163
R00-023	DNA prime with SeV-Gag boost	0			
R00-024	DNA prime with SeV-Gag boost	0			

acquire the potential for controlling SIVmac239 superchallenge. In the present study, we have examined whether these SHIV controllers acquired $CD8^+$ cells effective against SIVmac239 replication. Our analyses have suggested that $CD8^+$ cell responses capable of suppressing SIVmac239 replication in vitro were induced by controlled SHIV infection and that these responses might be crucial for control of superchallenged SIVmac239 replication.

MATERIALS AND METHODS

Animal experiments. Four Burmese rhesus macaques (*Macaca mulatta*) used in this study (Table 1) were maintained in accordance with the *Guides for Animal Experiments Performed at National Institute of Infectious Diseases* (35a). Blood collection, vaccination, virus challenge, and antibody administration were performed under ketamine anesthesia. These macaques received prophylactic vaccination and SHIV89.6PD challenge as described in our previous studies (27, 47). Macaque R00-017 was vaccinated intranasally with 1×10^8 cell infectious units (CIU) of replication-competent SeV-Gag vector (15, 16), whereas macaques R00-020, R00-023, and R00-024 were primed intramuscularly with 5 mg of cytomegalovirus (CMV)-SHIVdEN DNA and then boosted intranasally with 6×10^7 CIU of replication-defective F-deleted SeV-Gag vector (22). The CMV-SHIVdEN DNA was constructed from an *env*- and *nef*-deleted $SHIV_{MD14YE}$ molecular clone DNA (45) and has the genes encoding SIVmac239 Gag, Pol, Vif, and Vpx; SIVmac239-$HIV\text{-}1_{DH12}$ chimeric Vpr; and $HIV\text{-}1_{DH12}$ Tat and Rev as described previously (28, 47). These vaccinees were challenged intravenously with 10 50% tissue culture infective doses ($TCID_{50}$) of SHIV89.6PD (25) 13 weeks (in R00-020, R00-023, and R00-024) or 14 weeks (in R00-017) after SeV-Gag vaccination.

Macaques R00-023 and R00-024 were euthanized around 2 years after SHIV89.6PD challenge, while macaques R00-017 and R00-020 were followed up for more than 2 years. The latter two animals received monoclonal anti-CD20 antibody administration for $CD20^+$ cell depletion (starting at week 166 in R00-017 and week 140 in R00-020), intravenous superchallenge with 1,000 $TCID_{50}$ of SIVmac239 (18) (at week 203 in R00-017 and week 151 in R00-020), and monoclonal anti-CD8 antibody administration for $CD8^+$ cell depletion (starting at week 209 in R00-017 and week 163 in R00-020) (Table 1). For $CD20^+$ cell depletion, animals were inoculated intravenously with 10 mg/kg of monoclonal anti-CD20 antibody (Rituximab; Zenyaku Kogyo, Tokyo, Japan) four times every other week. Peripheral B-cell depletion was confirmed by immunostaining using anti-human CD19 antibody and anti-human CD20 antibody (Becton Dickinson, Tokyo, Japan). For $CD8^+$ cell depletion, animals received a single subcutaneous inoculation of 10 mg/kg of monoclonal anti-CD8 antibody (cM-T807) provided by Centocor (Malvern, PA) followed by three intravenous inoculations of 5 mg/kg cM-T807 on days 3, 7, and 10 after the first inoculation. Peripheral $CD8^+$ T-cell depletion was confirmed by immunostaining using anti-human CD8 antibody (DK25; Dako, Kyoto, Japan). Macaques R00-017 and R00-020 were euthanized 3 months after the anti-CD8 antibody administration.

Quantitation of plasma viral loads. Plasma RNA was extracted using the High Pure viral RNA kit (Roche Diagnostics, Tokyo, Japan). For quantitation of plasma SIV/SHIV RNA levels, serial fivefold dilutions of RNA samples were amplified in quadruplicate by reverse transcription (RT) and nested PCR to determine the endpoint. SIV *gag*-specific primers (AGAAACTCCGTCTTGT CAGG and TGATAATCTGCATAGCCGC for the first RT-PCR and GATTA GCAGAAAGCCTGTTGG and TGCAACCTTCTGACAGTGC for the second DNA PCR) (Sigma-Aldrich, Tokyo, Japan) that recognize the *gag* region shared by SHIV89.6PD and SIVmac239 were used. Plasma SIV/SHIV RNA levels were calculated according to the Reed-Muench method as described previously (28). The lower limit of detection in this assay is approximately 4×10^2 copies/ml. After SIVmac239 superchallenge, plasma SIVmac239 RNA levels were measured by the LightCycler system (Roche Diagnostics) using SIVmac239 *env*-specific primers (AAGAATTGTTGCGACTGACC and CAGTAGTGTGGCA GACTTGTC) and probes (CATTCAGCTGCGCCTGGTCCTTTAAGTAC-Flu and LcRed-TCTTCGATGGCAGTGACCCTAGTCTGGAGG) (Nihon Gene Research Laboratories, Inc., Sendai, Japan) that recognize SIVmac239 *env* but not SHIV89.6PD *env*. SHIV89.6PD RNA levels were also measured using SHIV89.6PD *env*-specific primers (GGATGTTGATGATCTGTAGTGC and CCAATACTACTTCTTGTGGGTT) and probes (CAGTCTATTATGGGG TACCTGTGTGGAGAGAAGCA-Flu and LcRed-CCACCACTCTATTTT GTGCATCAGATGCTAAAGCC) that recognize SHIV89.6PD *env* but not SIVmac239 *env*. The lower limit of detection in this assay is approximately 1×10^3 copies/ml.

In vitro viral suppression assay. We examined SIVmac239 replication on CD8-depleted peripheral blood mononuclear cells (PBMCs) in the presence of $CD8^+$ cells positively selected from PBMCs. Macaque PBMCs prepared from blood at several time points were frozen and stored until use. Thawed PBMCs were separated into $CD8^+$ cells and $CD8^-$ cells by using MACS CD8 MicroBeads (Miltenyi Biotec, Tokyo, Japan). The purity of the former was more than 96%, while the latter included less than 3% of $CD8^+$ cells. To prepare target cells, one fifth of $CD8^-$ cells negatively selected from PBMCs obtained before SHIV89.6PD challenge were infected with SIVmac239 at a multiplicity of infection (MOI) of $1:10^4$, and these infected cells and the remaining uninfected $CD8^-$ cells were cultured separately in the presence of 2 μg/ml phytohemagglutinin-L (Roche Diagnostics). After a 48-h culture, both infected and uninfected $CD8^-$ cells were collected, washed three times, and mixed to be used as target cells. Then, 4×10^3 target cells were cultured alone or cocultured with 4×10^5 (effector/target [E:T] ratio of 1:1) or 4×10^4 (E:T ratio of 1:10) $CD8^-$ effector cells positively selected from PBMCs in a well of 96-well flat-bottom plate and the culture supernatants were harvested every other day for measurement of SIV Gag CA p27 concentration by SIV core antigen enzyme-linked immunosorbent assay (ELISA) (Beckman Coulter, Tokyo, Japan). RPMI 1640 medium (Invitrogen, Tokyo, Japan) supplemented with 10% heat-inactivated fetal bovine serum (HyClone, Logan, UT) and 20 IU/ml recombinant human interleukin-2 (Roche Diagnostics) were used for cell culture. All of the cocultures were in duplicate, and the mean value of p27 concentrations at each time point is shown.

Measurement of virus-specific $CD8^+$ T-cell responses. We measured virus-specific T-cell levels by flow cytometric analysis of gamma interferon (IFN-γ) induction after specific stimulation as described previously (27, 28). PBMCs were cocultured with autologous herpesvirus papio-immortalized B-lymphoblastoid cell lines (B-LCL) (51) infected with vesicular stomatitis virus G (VSV-G)-pseudotyped SIVGP1 for SIVGP1-specific stimulation. The VSV-G-pseudotyped SIVGP1 was obtained by cotransfection of COS-1 cells with pVSV-G (Clontech, Otsu, Japan) and SIVGP1, an *env*- and *nef*-deleted $SHIV_{MD14}$ molecular clone DNA (28, 45). Intracellular IFN-γ staining was performed using a Cytofix-Cytoperm kit (Becton Dickinson). Peridinin chlorophyll-conjugated anti-human CD8, allophycocyanin-conjugated anti-human CD3, and phycoerythrin-conjugated anti-human IFN-γ antibodies (Becton Dickinson) were used. Specific T-cell levels were calculated by subtracting the IFN-γ T-cell frequencies after nonspecific stimulation from those after SIVGP1-specific stimulation.

Measurement of virus-specific neutralizing titers. We measured virus-specific neutralizing titers as described previously (17, 44). Serial twofold dilutions of heat-inactivated plasma were prepared in duplicate and mixed with 10 $TCID_{50}$ of SIVmac239 or SHIV89.6PD. In each mixture, 5 μl of diluted plasma was incubated with 5 μl of virus. After a 45-min incubation at room temperature, each 10-μl mixture was added to 5×10^4 MT-4 cells in a well of a 96-well flat-bottom

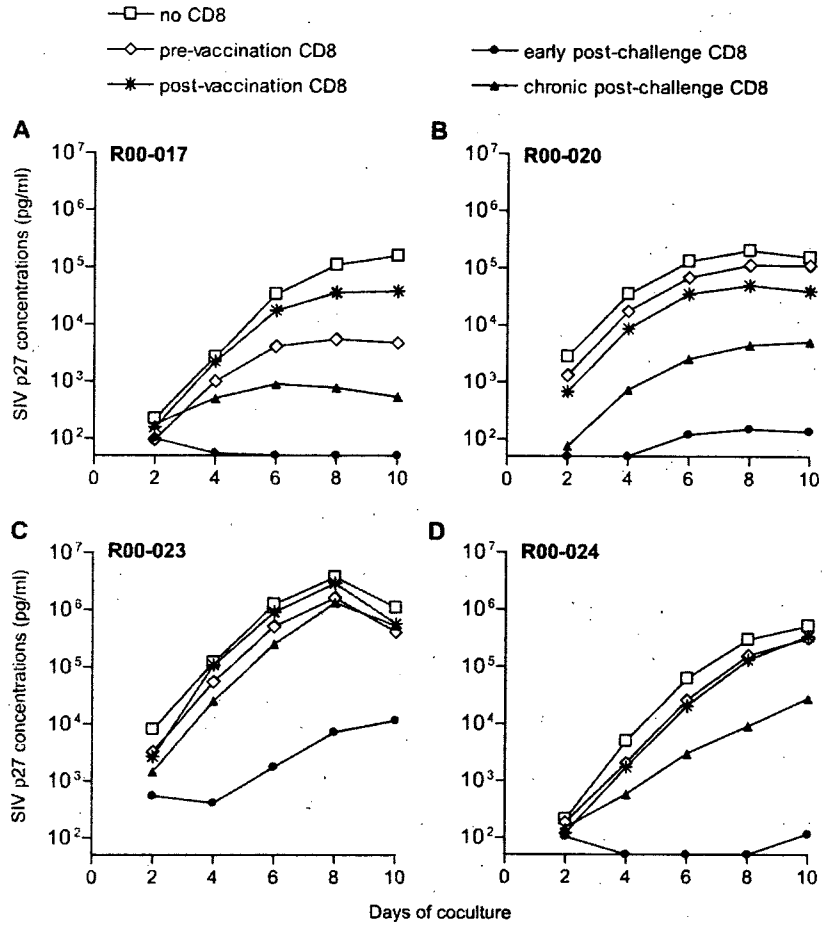

	R00-017	R00-020	R00-023	R00-024
post-vaccination	wks -6 & -4	wks -11 & -4	wk -7	wks -11 & -6
early post-challenge	wks 3 & 5	wks 5 & 8	wk 5	wks 5 & 13
chronic post-challenge	wk 67	wks 52 & 63	wk 30	wks 52 & 63

FIG. 1. SIVmac239 replication in vitro in the absence or the presence of $CD8^+$ cells in macaques R00-017 (A), R00-020 (B), R00-023 (C), and R00-024 (D). PBMC-derived $CD8^-$ (target) cells infected with SIVmac239 were cultured alone (no CD8) or cocultured with autologous PBMC-derived $CD8^-$ (effector) cells obtained prevaccination (pre-vaccination CD8), postvaccination and pre-SHIV challenge (post-vaccination CD8), in the early phase post-SHIV challenge (early post-challenge CD8), or in the chronic phase post-SHIV challenge (chronic post-challenge CD8) at an E:T ratio of 1:1. A representative result of two sets of experiments with similar patterns is shown in panels A and D, whereas the result of a single experiment is shown in panels B and C. Postvaccination and postchallenge $CD8^+$ cells were prepared from PBMCs obtained at different time points, as shown in the bottom table (weeks before [shown by minus] or after SHIV challenge), because of a limitation of available samples. SeV-Gag vaccination was performed 13 weeks (in R00-020, R00-023, and R00-024) or 14 weeks (in R00-017) before SHIV challenge. In some groups, CD8 cells at two time points were mixed to prepare enough cells. p27 concentrations in the culture supernatants were examined by ELISA.

plate. After 12 days of culture, supernatants were harvested. Progeny virus production in the supernatants was examined by SIV core antigen ELISA for detection of SIV p27 to determine the 100% neutralizing end point. The lower limit of detection is a titer of 1:2.

RESULTS

Potency of $CD8^+$ cells post-SHIV challenge for suppressing SIVmac239 replication in vitro. We established a method for examining SIVmac239 replication in vitro in the presence of $CD8^+$ cells and evaluated the effect of $CD8^+$ cells on SIVmac239 replication in vitro in four rhesus macaques that showed vaccine-based containment of SHIV89.6PD challenge (Table 1). One of them (R00-017) received a single intranasal SeV-Gag vaccination, while the other three (R00-020, R00-023, and R00-024) received a single intramuscular DNA priming followed by a single intranasal SeV-Gag booster before SHIV89.6PD challenge as described previously (27, 47). All four of these macaques controlled viral replication with undetectable plasma viremia after the acute phase for more than 2 years post-SHIV89.6PD challenge (54).

From each animal, we prepared four groups of bulk $CD8^+$ cells obtained prevaccination, post-SeV-Gag vaccination (pre-SHIV challenge), in the early phase post-SHIV challenge (weeks 3 to 8), and in the chronic phase post-SHIV challenge

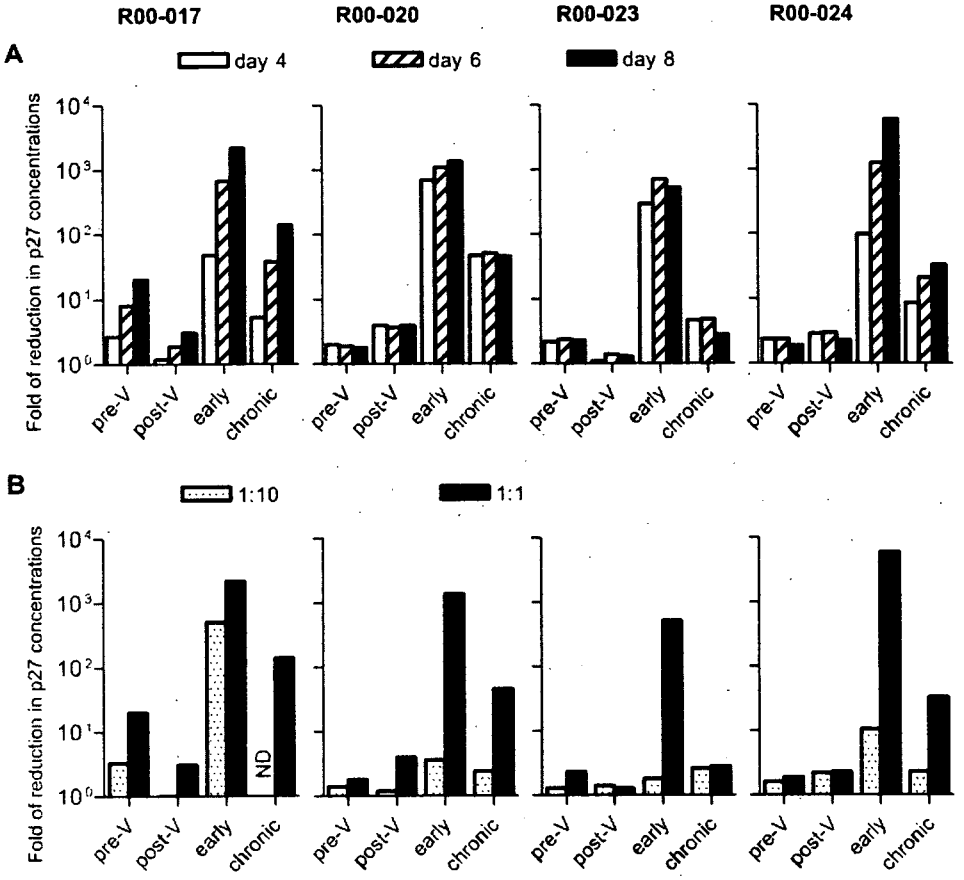

FIG. 2. Reduction in SIVmac239 production by addition of $CD8^+$ cells. The reduction (fold) in p27 concentration in the supernatant from coculture of SIV-infected $CD8^-$ cells with each group of $CD8^+$ cells compared to that from SIV-infected $CD8^-$ cell culture without $CD8^+$ cells is shown. (A) Reduction in p27 concentration on days 4, 6, and 8 of coculture at an E:T ratio of 1:1 (calculated from the data in Fig. 1). (B) Reduction in p27 concentration on day 8 of coculture at an E:T ratio of 1:1 (black bars) or 1:10 (dotted bars). pre-V, prevaccination CD8; post-V, postvaccination CD8; early, early postchallenge CD8; chronic, chronic postchallenge CD8 as described in the legend to Fig. 1. ND, not determined.

(weeks 30 to 67). These groups of effector $CD8^+$ cells were cocultured with SIVmac239-infected autologous target $CD8^-$ cells at the E:T ratio of 1:1, and p27 concentrations in the culture supernatants were measured for evaluation of SIVmac239 production (Fig. 1). Reduction in SIVmac239 production by addition of each group of $CD8^+$ cells was shown as reduction (fold) in p27 concentration compared to that in the supernatant from the SIVmac239-infected $CD8^-$ cell culture without $CD8^+$ cells (Fig. 2A).

Even addition of prevaccination $CD8^+$ cells resulted in reduction of SIV production. Especially, prevaccination $CD8^+$ cells derived from macaque R00-017 efficiently suppressed SIV replication, showing an approximately 20-fold reduction in viral production at day 8 of culture. In other three macaques, however, the reduction in SIV production by addition of prevaccination $CD8^+$ cells was less than threefold. In macaque R00-020, postvaccination/prechallenge $CD8^+$ cells suppressed SIV replication more efficiently than prevaccination ones, but in the other three macaques, the levels of suppression by postvaccination/prechallenge $CD8^+$ cells were not more than those by prevaccination cells.

In contrast, $CD8^+$ cells in the early phase postchallenge showed an efficient suppressive effect on SIV replication in all four macaques. Maximum reduction (fold) in SIV production by addition of these $CD8^+$ cells was more than 7×10^2. Addition of $CD8^+$ cells in the chronic phase postchallenge also resulted in efficient reduction of SIV production. The levels of reduction were lower than those by $CD8^+$ cells in the early phase postchallenge but higher than those by prechallenge $CD8^+$ cells. Thus, all four vaccinees, after SHIV challenge, acquired $CD8^+$ cells able to suppress SIVmac239 replication in vitro efficiently. Efficient reduction by early postchallenge $CD8^+$ cells was observed in some animals even at the E:T ratio of 1:10 (Fig. 2B).

We then measured SIVGP1-specific $CD8^+$ T-cell frequencies in PBMCs by detection of IFN-γ induction after stimulation with B-LCL expressing an *env*- and *nef*-deleted SHIV molecular clone (SIVGP1) DNA (27, 28) (Fig. 3). In all four macaques, SIVGP1-specific $CD8^+$ T-cell levels peaked during the acute phase post-SHIV challenge and gradually decreased after the set point. SIVGP1-specific $CD8^+$ T-cell frequencies after the acute phase were higher in macaques R00-017 and R00-023 compared to those post-SeV-Gag vaccination (prechallenge) but interestingly lower in macaque R00-020.

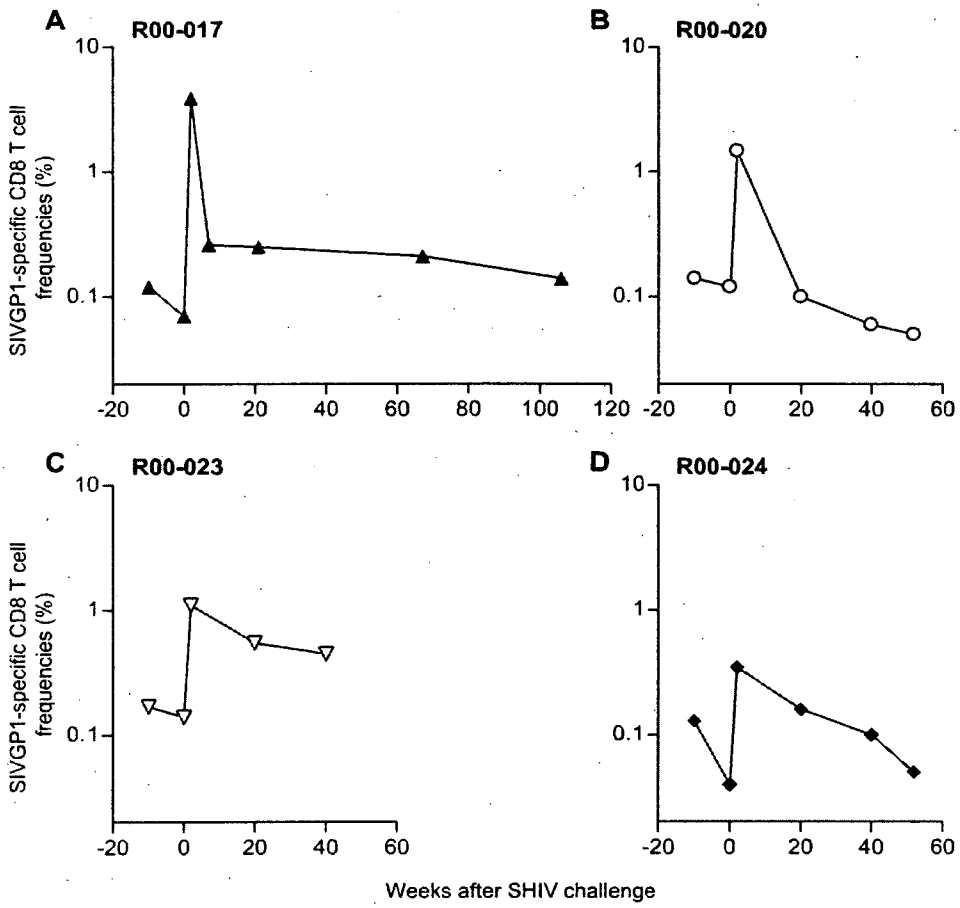

FIG. 3. SIVGP1-specific $CD8^+$ T-cell frequencies in macaques before and after SHIV89.6PD challenge. Frequencies of $CD8^+$ T cells showing SIVGP1-specific IFN-γ induction per total $CD8^+$ T cells in PBMCs are shown. The first time point prechallenge is 10 weeks before challenge.

CD20 depletion and SIVmac239 superchallenge in the SHIV controllers. Macaques R00-017 and R00-020 were further followed up and received monoclonal anti-CD20 antibody administration at week 166 (R00-017) or week 140 (R00-020) and SIVmac239 superchallenge at week 203 (R00-017) or week 151 (R00-020) (Table 1). Viral control was not abrogated, and plasma viremia remained undetectable after anti-CD20 antibody administration (Fig. 4). In both macaques, SHIV89.6PD-specific neutralizing antibodies (NAbs) were induced efficiently after SHIV89.6PD challenge and maintained at high levels in the chronic phase (54). The monoclonal anti-CD20 antibody administration resulted in rapid and prolonged depletion of peripheral $CD20^+$ lymphocytes, and more than a few months later, an approximately fourfold reduction in SHIV-specific NAb levels was observed (Fig. 5).

The following SIVmac239 superchallenge was contained in both macaques (Fig. 4). Macaque R00-017 did not show detectable plasma viremia even after SIVmac239 superchallenge, and macaque R00-020 showed only transient appearance of plasma viremia 1 week after SIVmac239 superchallenge. SIVmac239 *env* RNA but not SHIV89.6PD *env* RNA was detected in the transient plasma viremia (Fig. 6). SIVGP1-specific $CD8^+$ T-cell frequencies were at marginal levels just

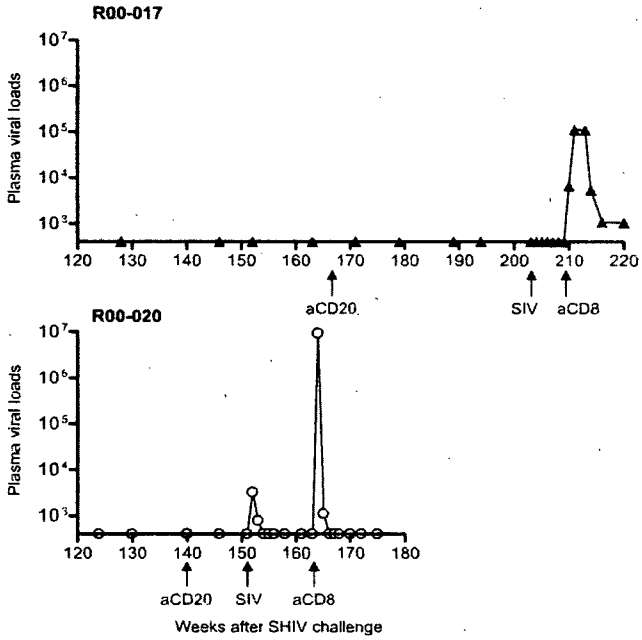

FIG. 4. Plasma viral loads (SIV *gag* RNA copies/ml plasma) in macaques R00-017 (upper panel) and R00-020 (lower panel) after week 120 post-SHIV challenge. aCD20 and aCD8, anti-CD20 and anti-CD8, respectively.

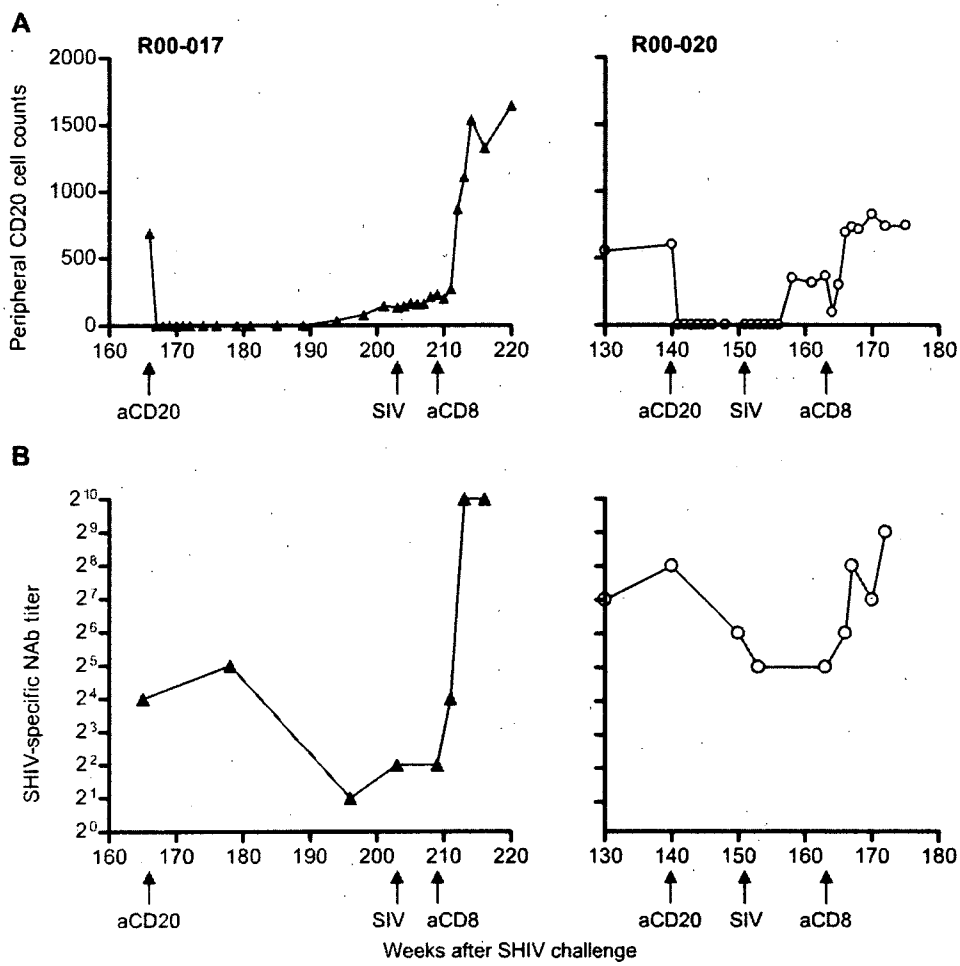

FIG. 5. Changes in SHIV89.6PD-specific NAb levels after monoclonal anti-CD20 antibody administration at week 166 in macaque R00-017 (left panels) and at week 140 in macaque R00-020 (right panels). (A) Peripheral $CD20^+$ cell counts (per μl). (B) SHIV89.6PD-specific neutralizing titers in plasma. aCD20 and aCD8, anti-CD20 and anti-CD8, respectively.

before SIVmac239 superchallenge but increased after the superchallenge (Fig. 7).

CD8 depletion after SIVmac239 superchallenge. Macaques R00-017 and R00-020 received monoclonal anti-CD8 antibody administration at week 209 (6 weeks after superchallenge) and week 163 (12 weeks after superchallenge), respectively (Table 1). Both macaques showed transient depletion of peripheral $CD8^+$ T lymphocytes and appearance of plasma viremia after the anti-CD8 antibody administration (Fig. 6).

In macaque R00-020, exhibiting a shorter period of $CD8^+$ T-lymphocyte depletion, plasma viremia was transient and detectable only at weeks 164 and 165, 1 and 2 weeks after the initial anti-CD8 antibody treatment. SIVmac239 *env* RNA but not SHIV89.6PD *env* RNA was detected in the transient plasma viremia. In macaque R00-017, exhibiting a longer period of $CD8^+$ T-lymphocyte depletion, plasma viremia appeared at week 210, 1 week after the initial anti-CD8 antibody treatment, and remained detectable during the observation period of 3 months. Interestingly, both SIVmac239 *env* RNA and SHIV89.6PD *env* RNA were detected; the former became detectable at week 210 and was detected during the observation period, whereas the latter was detected only at weeks 211 and 212. The former SIVmac239 *env* RNA levels peaked at week 213, and the latter SHIV89.6PD *env* RNA levels peaked at week 211.

SIVmac239-specific NAb responses were undetectable even after SIVmac239 superchallenge and CD8 depletion in both of the macaques (data not shown). SHIV89.6PD-specific NAb titers increased after the CD8 depletion not only in macaque R00-017 showing SHIV89.6PD viremia but also in macaque R00-020 without SHIV89.6PD viremia (Fig. 5). Both macaques showed increases in SIVGP1-specific $CD8^+$ T-cell frequencies after recovery from peripheral $CD8^+$ T-lymphocyte depletion (Fig. 7).

DISCUSSION

Previous $CD8^+$ cell depletion experiments in macaques using a monoclonal anti-CD8 antibody have indicated the importance of $CD8^+$ cell responses in SIV control in vivo (12, 29, 42). The present study evaluated the anti-SIV efficacy of these bulk $CD8^+$ cells in the vaccinated macaques that exhibited prophylactic SeV-Gag vaccine-based control of viral replication and showed induction of $CD8^+$ cells able to efficiently

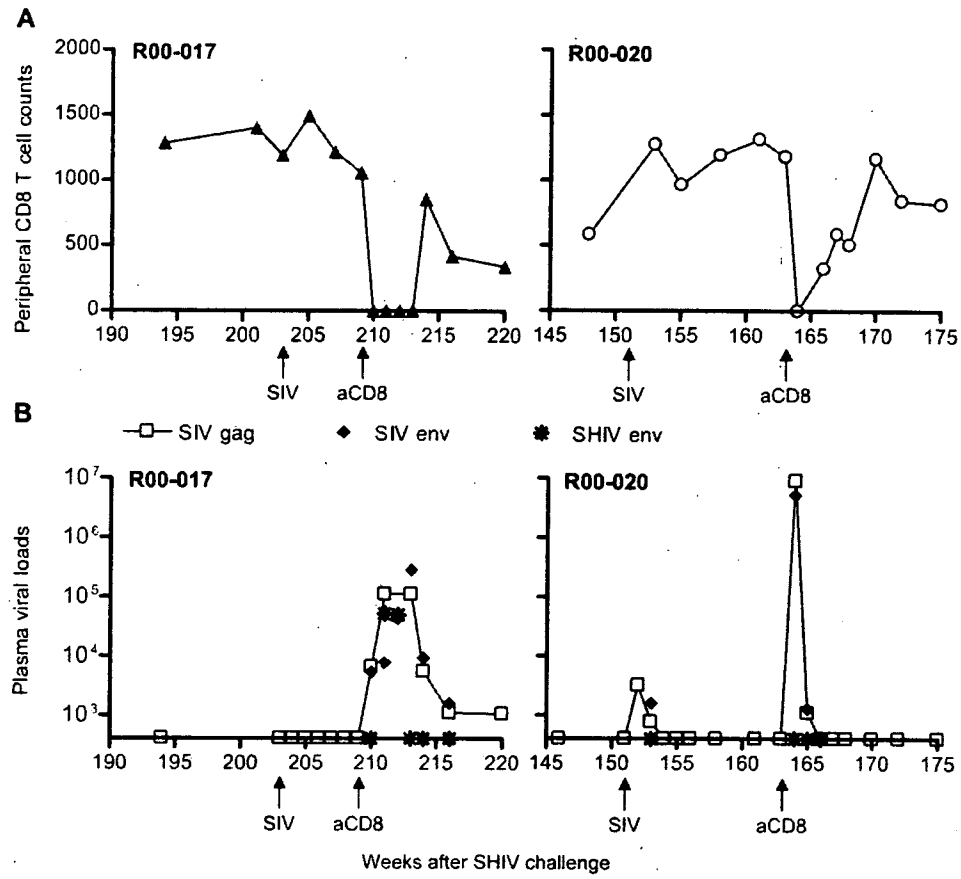

FIG. 6. SIVmac239 superchallenge and $CD8^+$ cell depletion in macaques R00-017 and R00-020. Macaque R00-017 received SIVmac239 superchallenge at week 203 and monoclonal anti-CD8 (aCD8) antibody administration starting at week 209, while macaque R00-020 received superchallenge at week 151 and anti-CD8 at week 163. (A) Peripheral $CD8^+$ T-cell counts (per μl) in macaques R00-017 (left panel) and R00-020 (right panel). (B) Plasma viral loads (copies/ml plasma) in macaques R00-017 (left panel) and R00-020 (right panel). In addition to SIV *gag* RNA levels, levels of SIV *env* RNA and SHIV *env* RNA at several time points are shown.

suppress SIV replication in vitro after SHIV challenge in these macaques. The difference in anti-SIV efficacies between postvaccination/prechallenge and postchallenge $CD8^+$ cells may explain why protective immune responses can be consistently induced not by current viral vector vaccination but by live virus infection.

These bulk $CD8^+$ cells are considered to include $CD8^+$ NK cells in addition to $CD8^+$ T lymphocytes. While previous studies using bulk $CD8^+$ cells or CTL clones (9, 24, 48, 55) have shown the importance of CTL activity on suppression of HIV/SIV replication, there may be a possibility that NK cells exert some suppressive effect on SIV replication, contributing to reductions in SIV production by prevaccination $CD8^+$ cells in the present study. The suppressive effect of postvaccination/prechallenge $CD8^+$ cells was not larger than that of prevaccination except for macaque R00-020. In contrast, postchallenge $CD8^+$ cells suppressed SIV replication more efficiently than those prevaccination and postvaccination. In the in vitro assay of SIV replication, individual macaques showed different sensitivities of target $CD8^+$ cells to SIV infection and different patterns of SIV replication kinetics in the absence of $CD8^+$ cells (Fig. 1). In macaque R00-023 showing higher levels of SIV production in the absence of $CD8^+$ cells, SIV infection at a lower MOI might exhibit a larger reduction in SIV production by addition of postchallenge $CD8^+$ cells.

Gag-specific $CD8^+$ T-cell levels peaked around 1 week after SeV-Gag vaccination and then decreased in the late phase after that (28). To prepare postvaccination/prechallenge $CD8^+$ cells, we used PBMCs in the late phase without those at week 1 post-SeV-Gag vaccination that include the peak levels of Gag-specific $CD8^+$ T cells. Thus, we compared anti-SIV efficacy of $CD8^+$ cells in the late phase postvaccination with that in the chronic phase post-SHIV challenge in this study. The postvaccination/prechallenge SIVGP1-specific $CD8^+$ T-cell frequencies roughly reflect Gag-specific $CD8^+$ T-cell ones because SIVGP1-specific $CD8^+$ T-cell responses were undetectable before SeV-Gag vaccination (data not shown). On the other hand, the postchallenge SIVGP1-specific $CD8^+$ T-cell responses are considered specific for SHIV antigens, including SIV-derived Gag, Pol, Vif, and partial Vpr. Therefore, our results shown in Fig. 3 suggest that SIV-specific $CD8^+$ T-cell frequencies in the chronic phase post-SHIV challenge were less than those post-SeV-Gag vaccination (prechallenge) in macaque R00-020. Interestingly, however, such postchallenge $CD8^+$ cells suppressed SIV replication more efficiently than postvaccination/prechallenge ones. Thus, SIV-specific $CD8^+$

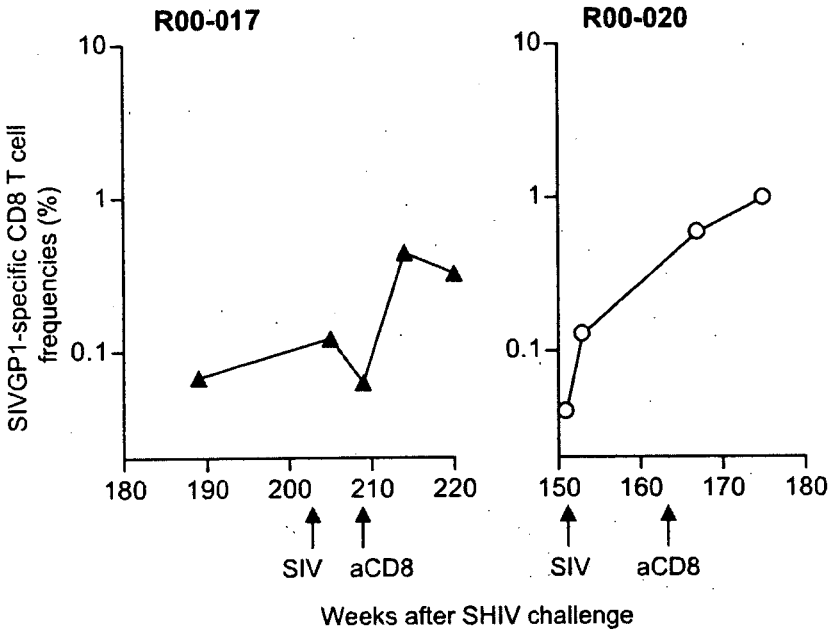

FIG. 7. SIVGP1-specific $CD8^+$ T-cell frequencies in macaques R00-017 (left panel) and R00-020 (right panel) before and after SIVmac239 superchallenge. Frequencies of $CD8^+$ T cells showing SIVGP1-specific IFN-γ induction per total $CD8^+$ T cells in PBMCs are shown. aCD8, anti-CD8.

T-cell frequencies may not always correlate with anti-SIV efficacy in vitro. It may be because postchallenge-induced, certain epitope-specific $CD8^+$ T cells may have higher anti-SIV efficacy in vitro than postvaccination/prechallenge $CD8^+$ T cells in this macaque. There may be a possibility of augmentation of anti-SIV efficacy by induction of broader $CD8^+$ T-cell responses after SHIV challenge.

A previous $CD8^+$ cell depletion study in macaques infected with live attenuated SIV has shown partial loss of superchallenged SIVmac251 control by monoclonal anti-CD8 antibody administration at the superchallenge and has suggested involvement of both cellular and humoral immune responses in this control (43). On the other hand, administration of monoclonal anti-CD8 antibody to macaques infected with live attenuated SIVmac239Δnef after SIVmac251 superchallenge resulted in the appearance of SIVmac239Δnef viremia without detectable SIVmac251 viremia (33). In contrast, the present study showed the appearance of superchallenged SIVmac239 viremia by monoclonal anti-CD8 antibody administration after superchallenge, suggesting that $CD8^+$ cells were crucial for the control of superchallenged SIVmac239 replication. It can be speculated that, in SIVmac239Δnef-infected animals, live virus replication levels before superchallenge were higher, resulting in more strict containment of superchallenge than that in our study. Additionally, neutralizing antibody responses may be involved in the containment of superchallenge in SIVmac239Δnef-infected animals but not in SHIV-infected ones. Thus, our results imply a more profound contribution of $CD8^+$ cells to control of SIV superchallenge in the absence of NAb help.

More than a few months after the anti-CD20 antibody administration, both macaques R00-017 and R00-020 showed fourfold reductions in SHIV-specific neutralizing titers, although it is unclear if these reductions were due to the $CD20^+$ cell depletion. Macaque R00-017 with a lower neutralizing titer showed transient appearance of SHIV viremia by $CD8^+$ cell depletion, but macaque R00-020 with a higher titer did not. These results were consistent with the previous study indicating involvement of humoral as well as cellular immune responses in the CXCR4-tropic SHIV control (26).

In summary, our results indicate that $CD8^+$ cells acquired the ability to efficiently suppress CCR5-tropic SIV replication in vitro by controlled CXCR4-tropic SHIV infection. While the levels of in vitro anti-SIV efficacy resulting in SIV control in vivo have not been determined, our results imply that such $CD8^+$ cell responses may be crucial for live attenuated vaccine-based containment of HIV/SIV superinfection.

ACKNOWLEDGMENTS

This work was supported by a grant from the Ministry of Education, Culture, Sports, Science, and Technology; grants from the Japan Health Sciences Foundation; and grants from the Ministry of Health, Labor, and Welfare in Japan.

The animal experiments were conducted through the Cooperative Research Program at the Tsukuba Primate Research Center, National Institute of Biomedical Innovation, with the help of the Corporation for Production and Research of Laboratory Primates. We thank Centocor, Inc., and K. A. Reimann for providing cM-T807 and M. Takiguchi, F. Ono, K. Komatsuzaki, A. Hiyaoka, A. Oyama, K. Oto, H. Akari, K. Terao, M. Miyazawa, A. Kimura, K. Mori, N. Yamamoto, T. Sata, T. Kurata, Y. Nagai, and A. Nomoto for their help.

REFERENCES

1. **Altfeld, M., and E. S. Rosenberg.** 2000. The role of $CD4^+$ T helper cells in the cytotoxic T lymphocyte response to HIV-1. Curr. Opin. Immunol. **12**: 375–380.
2. **Amara, R. R., F. Villinger, J. D. Altman, S. L. Lydy, S. P. O'Neil, S. I. Staprans, D. C. Montefiori, Y. Xu, J. G. Herndon, L. S. Wyatt, M. A.**

Candido, N. L. Kozyr, P. L. Earl, J. M. Smith, H. L. Ma, B. D. Grimm, M. L. Hulsey, J. Miller, H. M. McClure, J. M. McNicholl, B. Moss, and H. L. Robinson. 2001. Control of a mucosal challenge and prevention of AIDS in rhesus macaques by a multiprotein DNA/MVA vaccine. Science **292**:69–74.

3. **Baba, T. W., Y. S. Jeong, D. Pennick, R. Bronson, M. F. Greene, and R. M. Ruprecht.** 1995. Pathogenicity of live, attenuated SIV after mucosal infection of neonatal macaques. Science **267**:1820–1825.
4. **Borrow, P., H. Lewicki, B. H. Hahn, G. M. Shaw, and M. B. A. Oldstone.** 1994. Virus-specific $CD8^+$ cytotoxic T-lymphocyte activity associated with control of viremia in primary human immunodeficiency virus type 1 infection. J. Virol. **68**:6103–6110.
5. **Brander, C., and B. D. Walker.** 1999. T lymphocyte responses in HIV-1 infection: implication for vaccine development. Curr. Opin. Immunol. **11**: 451–459.
6. **Casimiro, D. R., F. Wang, W. A. Schleif, X. Liang, Z.-Q. Zhang, T. W. Tobery, M.-E. Davies, A. B. McDermott, D. H. O'Connor, A. Fridman, A. Bagchi, L. G. Tussey, A. J. Bett, A. C. Finnefrock, T.-M. Fu, A. Tang, K. A. Wilson, M. Chen, H. C. Perry, G. J. Heidecker, D. C. Freed, A. Carella, K. S. Punt, K. J. Sykes, L. Huang, V. I. Ausensi, M. Bachinsky, U. Sadasivan-Nair, D. I. Watkins, E. A. Emini, and J. W. Shiver.** 2005. Attenuation of simian immunodeficiency virus SIVmac239 infection by prophylactic immunization with DNA and recombinant adenoviral vaccine vectors expressing Gag. J. Virol. **79**:15547–15555.
7. **Daniel, M. D., F. Kirchhoff, S. C. Czajak, P. K. Sehgal, and R. C. Desrosiers.** 1992. Protective effects of a live attenuated SIV vaccine with a deletion in the nef gene. Science **258**:1938–1941.
8. **Feinberg, M. B., and J. P. Moore.** 2002. AIDS vaccine models: challenging challenge viruses. Nat. Med. **8**:207–210.
9. **Gauduin, M.-C., R. L. Glickman, R. Means, and R. P. Johnson.** 1998. Inhibition of simian immunodeficiency virus (SIV) replication by $CD8^+$ T lymphocytes from macaques immunized with live attenuated SIV. J. Virol. **72**:6315–6324.
10. **Goulder, P. J., and D. I. Watkins.** 2004. HIV and SIV CTL escape: implications for vaccine design. Nat. Rev. Immunol. **4**:630–640.
11. **Horton, H., T. U. Vogel, D. K. Carter, K. Vielhuber, D. H. Fuller, T. Shipley, J. T. Fuller, K. J. Kunstman, G. Sutter, D. C. Montefiori, V. Erfle, R. C. Desrosiers, N. Wilson, L. J. Picker, S. M. Wolinsky, C. Wang, D. B. Allison, and D. I. Watkins.** 2002. Immunization of rhesus macaques with a DNA prime/modified vaccinia virus Ankara boost regimen induces broad simian immunodeficiency virus (SIV)-specific T-cell responses and reduces initial viral replication but does not prevent disease progression following challenge with pathogenic SIVmac239. J. Virol. **76**:7187–7202.
12. **Jin, X., D. E. Bauer, S. E. Tuttleton, S. Lewin, A. Gettie, J. Blanchard, C. E. Irwin, J. T. Safrit, J. Mittler, L. Weinberger, L. G. Kostrikis, L. Zhang, A. S. Perelson, and D. D. Ho.** 1999. Dramatic rise in plasma viremia after CD8+ T cell depletion in simian immunodeficiency virus-infected macaques. J. Exp. Med. **189**:991–998.
13. **Johnson, R. P., and R. C. Desrosiers.** 1998. Protective immunity induced by live attenuated simian immunodeficiency virus. Curr. Opin. Immunol. **10**: 436–443.
14. **Johnson, R. P., J. D. Lifson, S. C. Czajak, K. S. Cole, K. H. Manson, R. Glickman, J. Yang, D. C. Montefiori, R. Montelaro, M. S. Wyand, and R. C. Desrosiers.** 1999. Highly attenuated vaccine strains of simian immunodeficiency virus protect against vaginal challenge: inverse relationship of degree of protection with level of attenuation. J. Virol. **73**:4952–4961.
15. **Kano, M., T. Matano, A. Kato, H. Nakamura, A. Takeda, Y. Suzaki, Y. Ami, K. Terao, and Y. Nagai.** 2002. Primary replication of a recombinant Sendai virus vector in macaques. J. Gen. Virol. **83**:1377–1386.
16. **Kato, A., Y. Sakai, T. Shioda, T. Kondo, M. Nakanishi, and Y. Nagai.** 1996. Initiation of Sendai virus multiplication from transfected cDNA or RNA with negative or positive sense. Genes Cells **1**:569–579.
17. **Kawada, M., T. Tsukamoto, H. Yamamoto, A. Takeda, H. Igarashi, D. I. Watkins, and T. Matano.** 2007. Long-term control of simian immunodeficiency virus replication with central memory $CD4^+$ T-cell preservation after nonsterile protection by a cytotoxic T-lymphocyte-based vaccine. J. Virol. **81**:5202–5211.
18. **Kestler, H. W., III, D. J. Ringler, K. Mori, D. L. Panicali, P. K. Sehgal, M. D. Daniel, and R. C. Desrosiers.** 1991. Importance of the nef gene for maintenance of high virus loads and for development of AIDS. Cell **65**:651–662.
19. **Koff, W. C., P. R. Johnson, D. I. Watkins, D. R. Burton, J. D. Lifson, K. J. Hasenkrug, A. B. McDermott, A. Schultz, T. J. Zamb, R. Boyle, and R. C. Desrosiers.** 2006. HIV vaccine design: insights from live attenuated SIV vaccines. Nat. Immunol. **7**:19–23.
20. **Koup, R. A., J. T. Safrit, Y. Cao, C. A. Andrews, G. McLeod, W. Borkowsky, C. Farthing, and D. D. Ho.** 1994. Temporal association of cellular immune responses with the initial control of viremia in primary human immunodeficiency virus type 1 syndrome. J. Virol. **68**:4650–4655.
21. **Letvin, N. L., J. R. Mascola, Y. Sun, D. A. Gorgone, A. P. Buzby, L. Xu, Z. Y. Yang, B. Chakrabarti, S. S. Rao, J. E. Schmitz, D. C. Montefiori, B. R. Barker, F. L. Bookstein, and G. J. Nabel.** 2006. Preserved CD4+ central memory T cells and survival in vaccinated SIV-challenged monkeys. Science **312**:1530–1533.
22. **Li, H.-O., Y.-F. Zhu, M. Asakawa, H. Kuma, T. Hirata, Y. Ueda, Y.-S. Lee, M. Fukumura, A. Iida, A. Kato, Y. Nagai, and M. Hasegawa.** 2000. A cytoplasmic RNA vector derived from nontransmissible Sendai virus with efficient gene transfer and expression. J. Virol. **74**:6564–6569.
23. **Li, Q., L. Duan, J. D. Estes, Z. M. Ma, T. Rourke, Y. Wang, C. Reilly, J. Carlis, C. J. Miller, and A. T. Haase.** 2005. Peak SIV replication in resting memory CD4+ T cells depletes gut lamina propria CD4+ T cells. Nature **434**:1148–1152.
24. **Loffredo, J. T., E. G. Rakasz, J. P. Giraldo, S. P. Spencer, K. K. Grafton, S. R. Martin, G. Napoé, L. J. Yant, N. A. Wilson, and D. I. Watkins.** 2005. $Tat_{28-35}SL8$-specific $CD8^+$ T lymphocytes are more effective than $Gag_{181-189}CM9$-specific $CD8^+$ T lymphocytes at suppressing simian immunodeficiency virus replication in a functional in vitro assay. J. Virol. **79**:14986–14991.
25. **Lu, Y., C. D. Pauza, X. Lu, D. C. Montefiori, and C. J. Miller.** 1998. Rhesus macaques that become systemically infected with pathogenic SHIV 89.6-PD after intravenous, rectal, or vaginal inoculation and fail to make an antiviral antibody response rapidly develop AIDS. J. Acquir. Immune Defic. Syndr. Hum. Retrovirol. **19**:6–18.
26. **Mao, H., B. A. P. Lafont, T. Igarashi, Y. Nishimura, C. Brown, V. Hirsch, A. Buckler-White, R. Sadjadpour, and M. A. Martin.** 2005. $CD8^+$ and $CD20^+$ lymphocytes cooperate to control acute simian immunodeficiency virus/human immunodeficiency virus chimeric virus infections in rhesus monkeys: modulation by major histocompatibility complex genotype. J. Virol. **79**:14887–14898.
27. **Matano, T., M. Kano, H. Nakamura, A. Takeda, and Y. Nagai.** 2001. Rapid appearance of secondary immune responses and protection from acute CD4 depletion after a highly pathogenic immunodeficiency virus challenge in macaques vaccinated with a DNA prime/Sendai viral vector boost regimen. J. Virol. **75**:11891–11896.
28. **Matano, T., M. Kobayashi, H. Igarashi, A. Takeda, H. Nakamura, M. Kano, C. Sugimoto, K. Mori, A. Iida, T. Hirata, M. Hasegawa, T. Yuasa, M. Miyazawa, Y. Takahashi, M. Yasunami, A. Kimura, D. H. O'Connor, D. I. Watkins, and Y. Nagai.** 2004. Cytotoxic T lymphocyte-based control of simian immunodeficiency virus replication in a preclinical AIDS vaccine trial. J. Exp. Med. **199**:1709–1718.
29. **Matano, T., R. Shibata, C. Siemon, M. Connors, H. C. Lane, and M. A. Martin.** 1998. Administration of an anti-CD8 monoclonal antibody interferes with the clearance of chimeric simian/human immunodeficiency virus during primary infections of rhesus macaques. J. Virol. **72**:164–169.
30. **Mattapallil, J. J., D. C. Douek, A. Buckler-White, D. C. Montefiori, N. L. Letvin, G. J. Nabel, and M. Roederer.** 2006. Vaccination preserves CD4 memory T cells during acute simian immunodeficiency virus challenge. J. Exp. Med. **203**:1533–1541.
31. **Mattapallil, J. J., D. C. Douek, B. Hill, Y. Nishimura, M. A. Martin, and M. Roederer.** 2005. Massive infection and loss of memory CD4+ T cells in multiple tissues during acute SIV infection. Nature **434**:1093–1097.
32. **McMichael, A. J., and T. Hanke.** 2003. HIV vaccines 1983–2003. Nat. Med. **9**:874–880.
33. **Metzner, K. J., X. Jin, F. V. Lee, A. Gettie, D. E. Bauer, M. D. Mascio, A. S. Perelson, P. A. Marx, D. D. Ho, L. G. Kostrikis, and R. I. Connor.** 1999. Effects of in vivo CD8+ T cell depletion on virus replication in rhesus macaques immunized with a live, attenuated simian immunodeficiency virus vaccine. J. Exp. Med. **191**:1921–1932.
34. **Miller, C. J., and K. Abel.** 2005. Immune mechanisms associated with protection from vaginal SIV challenge in rhesus monkeys infected with virulence-attenuated SHIV 89.6. J. Med. Primatol. **34**:271–281.
35. **Miller, C. J., M. B. McChesney, X. Lü, P. J. Dailey, C. Chutkowski, D. Lu, P. Brosio, B. Roberts, and Y. Lu.** 1997. Rhesus macaques previously infected with simian/human immunodeficiency virus are protected from vaginal challenge with pathogenic SIVmac239. J. Virol. **71**:1911–1921.

35a. **National Institute of Infectious Diseases.** 2007. Guides for animal experiments performed at National Institute of Infectious Diseases. National Institute of Infectious Diseases, Tokyo, Japan. (In Japanese).

36. **Nishimura, Y., C. R. Brown, J. J. Mattapallil, T. Igarashi, A. Buckler-White, B. A. Lafont, V. M. Hirsch, M. Roederer, and M. A. Martin.** 2005. Resting naive CD4+ T cells are massively infected and eliminated by X4-tropic simian-human immunodeficiency viruses in macaques. Proc. Natl. Acad. Sci. USA **102**:8000–8005.
37. **Nishimura, Y., T. Igarashi, O. K. Donau, A. Buckler-White, C. Buckler, B. A. Lafont, R. M. Goeken, S. Goldstein, V. M. Hirsch, and M. A. Martin.** 2004. Highly pathogenic SHIVs and SIVs target different CD4+ T cell subsets in rhesus monkeys, explaining their divergent clinical courses. Proc. Natl. Acad. Sci. USA **101**:12324–12329.
38. **Ogg, G. S., X. Jin, S. Bonhoeffer, P. R. Dunbar, M. A. Nowak, S. Monard, J. P. Segal, Y. Cao, S. L. Rowland-Jones, V. Cerundolo, A. Hurley, M. Markowitz, D. D. Ho, D. F. Nixon, and A. J. McMichael.** 1998. Quantitation of HIV-1-specific cytotoxic T lymphocytes and plasma load of viral RNA. Science **279**:2103–2106.
39. **Picker, L. J., and D. I. Watkins.** 2005. HIV pathogenesis: the first cut is the deepest. Nat. Immunol. **6**:430–432.
40. **Rose, N. F., P. A. Marx, A. Luckay, D. F. Nixon, W. J. Moretto, S. M. Donahoe, D. Montefiori, A. Roberts, L. Buonocore, and J. K. Rose.** 2001. An

effective AIDS vaccine based on live attenuated vesicular stomatitis virus recombinants. Cell **106**:539–549.
41. **Rosenberg, E. S., J. M. Billingsley, A. M. Caliendo, S. L. Boswell, P. E. Sax, S. A. Kalams, and B. D. Walker.** 1997. Vigorous HIV-1-specific CD4$^+$ T cell responses associated with control of viremia. Science **278**:1447–1450.
42. **Schmitz, J. E., M. J. Kuroda, S. Santra, V. G. Sasseville, M. A. Simon, M. A. Lifton, P. Racz, K. Tenner-Racz, M. Dalesandro, B. J. Scallon, J. Ghrayeb, M. A. Forman, D. C. Montefiori, E. P. Rieber, N. L. Letvin, and K. A. Reimann.** 1999. Control of viremia in simian immunodeficiency virus infection by CD8+ lymphocytes. Science **283**:857–860.
43. **Schmitz, J. E., R. P. Johnson, H. M. McClure, K. H. Manson, M. S. Wyand, M. J. Kuroda, M. A. Lifton, R. S. Khunkhun, K. J. McEvers, J. Gillis, M. Piatak, J. D. Lifson, G. Grosschupff, P. Racz, K. Tenner-Racz, E. P. Rieber, K. Kuus-Reichel, R. S. Gelman, N. L. Letvin, D. C. Montefiori, R. M. Ruprecht, R. C. Desrosiers, and K. A. Reimann.** 2005. Effect of CD8$^+$ lymphocyte depletion on virus containment after simian immunodeficiency virus SIVmac251 challenge of live attenuated SIVmac239Δ3-vaccinated rhesus macaques. J. Virol. **79**:8131–8141.
44. **Shibata, R., C. Siemon, S. C. Czajak, R. C. Desrosiers, and M. A. Martin.** 1997. Live, attenuated simian immunodeficiency virus vaccines elicit potent resistance against a challenge with a human immunodeficiency virus type 1 chimeric virus. J. Virol. **71**:8141–8148.
45. **Shibata, R., F. Maldarelli, C. Siemon, T. Matano, M. Parta, G. Miller, T. Fredrickson, and M. A. Martin.** 1997. Infection and pathogenicity of chimeric simian-human immunodeficiency viruses in macaques: determinants of high virus loads and CD4 cell killing. J. Infect. Dis. **176**:362–373.
46. **Shiver, J. W., T. M. Fu, L. Chen, D. R. Casimiro, M. E. Davies, R. K. Evans, Z. Q. Zhang, A. J. Simon, W. L. Trigona, S. A. Dubey, L. Huang, V. A. Harris, R. S. Long, X. Liang, L. Handt, W. A. Schleif, L. Zhu, D. C. Freed, N. V. Persaud, L. Guan, K. S. Punt, A. Tang, M. Chen, K. A. Wilson, K. B. Collins, G. J. Heidecker, V. R. Fernandez, H. C. Perry, J. G. Joyce, K. M. Grimm, J. C. Cook, P. M. Keller, D. S. Kresock, H. Mach, R. D. Troutman, L. A. Isopi, D. M. Williams, Z. Xu, K. E. Bohannon, D. B. Volkin, D. C. Montefiori, A. Miura, G. R. Krivulka, M. A. Lifton, M. J. Kuroda, J. E. Schmitz, N. L. Letvin, M. J. Caulfield, A. J. Bett, R. Youil, D. C. Kaslow, and E. A. Emini.** 2002. Replication-incompetent adenoviral vaccine vector elicits effective anti-immunodeficiency-virus immunity. Nature **415**:331–335.
47. **Takeda, A., H. Igarashi, H. Nakamura, M. Kano, A. Iida, T. Hirata, M. Hasegawa, Y. Nagai, and T. Matano.** 2003. Protective efficacy of an AIDS vaccine, a single DNA priming followed by a single booster with a recombinant replication-defective Sendai virus vector, in a macaque AIDS model. J. Virol. **77**:9710–9715.
48. **Tomiyama, H., M. Fujiwara, S. Oka, and M. Takiguchi.** 2005. Epitope-dependent effect of Nef-mediated HLA class I down-regulation on ability of HIV-1-specific CTLs to suppress HIV-1 replication. J. Immunol. **174**:36–40.
49. **Veazey, R. S., K. G. Mansfield, I. C. Tham, A. C. Carville, D. E. Shvetz, A. E. Forand, and A. A. Lackner.** 2000. Dynamics of CCR5 expression by CD4$^+$ T cells in lymphoid tissues during simian immunodeficiency virus infection. J. Virol. **74**:11001–11007.
50. **Veazey, R. S., M. DeMaria, L. V. Chalifoux, D. E. Shvetz, D. R. Pauley, H. L. Knight, M. Rosenzweig, R. P. Johnson, R. C. Desrosiers, and A. A. Lackner.** 1998. Gastrointestinal tract as a major site of CD4+ T cell depletion and viral replication in SIV infection. Science **280**:427–431.
51. **Voss, G., S. Nick, C. Stahl-Hennig, K. Ritter, and G. Hunsmann.** 1992. Generation of macaque B lymphoblastoid cell lines with simian Epstein-Barr-like viruses: transformation procedure, characterization of the cell lines and occurrence of simian foamy virus. J. Virol. Methods **39**:185–195.
52. **Wilson, N. A., J. Reed, G. S. Napoe, S. Piaskowski, A. Szymanski, J. Furlott, E. J. Gonzalez, L. J. Yant, N. J. Maness, G. E. May, T. Soma, M. R. Reynolds, E. Rakasz, R. Rudersdorf, A. B. McDermott, D. H. O'Connor, T. C. Friedrich, D. B. Allison, A. Patki, L. J. Picker, D. R. Burton, J. Lin, L. Huang, D. Patel, G. Heindecker, J. Fan, M. Citron, M. Horton, F. Wang, X. Liang, J. W. Shiver, D. R. Casimiro, and D. I. Watkins.** 2006. Vaccine-induced cellular immune responses reduce plasma viral concentrations after repeated low-dose challenge with pathogenic simian immunodeficiency virus SIVmac239. J. Virol. **80**:5875–5885.
53. **Wyand, M. S., K. H. Manson, M. Garcia-Moll, D. C. Montefiori, and R. C. Desrosiers.** 1996. Vaccine protection by a triple deletion mutant of simian immunodeficiency virus. J. Virol. **70**:3724–3733.
54. **Yamamoto, H., M. Kawada, T. Tsukamoto, A. Takeda, H. Igarashi, M. Miyazawa, T. Naruse, M. Yasunami, A. Kimura, and T. Matano.** 2007. Vaccine-based, long-term, stable control of simian/human immunodeficiency virus 89.6PD replication in rhesus macaques. J. Gen. Virol. **88**:652–659.
55. **Yang, O. O., S. A. Kalams, A. Trocha, H. Cao, A. Luster, R. P. Johnson, and B. D. Walker.** 1997. Suppression of human immunodeficiency virus type 1 replication by CD8$^+$ cells: evidence for HLA class I-restricted triggering of cytolytic and noncytolytic mechanisms. J. Virol. **71**:3120–3128.

ELSEVIER

INSTITUT PASTEUR

Microbes and Infection 9 (2007) 1590–1596

www.elsevier.com/locate/micinf

Original article

Inhibition of infectious murine leukemia virus production by *Fv-4 env* gene products exerting dominant negative effect on viral envelope glycoprotein

Akiko Takeda [a], Tetsuro Matano [a,b,*]

[a] *International Research Center for Infectious Diseases, The Institute of Medical Science, The University of Tokyo, 4-6-1 Shirokanedai, Minato-ku, Tokyo 108-8639, Japan*

[b] *AIDS Research Center, National Institute of Infectious Diseases, 1-23-1 Toyama, Shinjuku-ku, Tokyo 162-8640, Japan*

Received 5 August 2007; accepted 9 September 2007

Available online 23 September 2007

Abstract

Fv-4 is a mouse gene that confers resistance against ecotropic murine leukemia virus (MLV) infection on mice. While receptor interference by the *Fv-4 env* gene product, Fv-4 Env, that can bind to the ecotropic MLV receptor has been shown to play an important role in the resistance, other mechanisms have also been suggested because it confers extremely efficient, complete resistance in vivo. Here, we have examined the effect of Fv-4 Env on infectious MLV production. Infectious MLV titers in supernatants obtained after transfection with a Friend MLV (FMLV) Env-expressing plasmid from MLV *gag–pol* producer cells harboring a retroviral vector were largely reduced by coexpression of Fv-4 Env. Syncytia formation mediated by R-peptide-deleted FMLV Env in NIH 3T3 cells was impaired by Fv-4 Env coexpression. Similarly, Fv-4 Env inhibited infectious amphotropic MLV production and syncytia formation mediated by R-peptide-deleted amphotropic MLV Env. Immunoprecipitation analysis revealed interaction of Fv-4 Env with amphotropic MLV Env as well as FMLV Env. These results indicate that Fv-4 Env inhibits infectious ecotropic and amphotropic MLV production by exerting dominant negative effect on MLV Env, suggesting contribution of this inhibitory effect to the resistance against ecotropic MLV infection in *Fv-4*-expressing mice.

Keywords: MLV; Fv-4; Env

1. Introduction

The *Fv-4* locus has been identified as a dominant gene that confers resistance to Friend virus-induced disease in mice [1]. *Fv-4* corresponds to a defective endogenous provirus with an ecotropic murine leukemia virus (MLV)-like *env* gene [2,3]. The *Fv-4 env* gene product, Fv-4 Env, having approximately 70% amino acid sequence homology with ecotropic Moloney MLV (MoMLV) and Friend MLV (FMLV) Envs has been shown to bind to the ecotropic MLV receptor and inhibit entry of ecotropic MLV into the cells [2,4]. Such receptor interference has been indicated to play an important role in the resistance to Friend virus infection [2]. While contribution of immune responses to this resistance has also been indicated, additional mechanisms have been suggested because *Fv-4* confers extremely efficient, complete resistance in vivo [5–10]. Elucidation of such natural resistance mechanism may lead to development of a strategy against viral infection.

MLVs are divided into several groups such as ecotropic, amphotropic, and xenotropic MLVs according to their receptor usage [11]. The receptor-binding domain locates in the amino (N)-terminal half of Env SU (surface subunit) [12–15]. MLV Envs are oligomerized to form trimers in the endoplasmic reticulum, processed into SU and TM (transmembrane subunit)

* Corresponding author. International Research Center for Infectious Diseases, The Institute of Medical Science, The University of Tokyo, 4-6-1 Shirokanedai, Minato-ku, Tokyo 108-8639, Japan. Tel.: +81 3 6409 2078; fax: +81 3 6409 2076.

E-mail address: matano@m.u-tokyo.ac.jp (T. Matano).

1286-4579/$ - see front matter © 2007 Elsevier Masson SAS. All rights reserved.
doi:10.1016/j.micinf.2007.09.012

in the Golgi apparatus, expressed on the cell surface, and incorporated into the virion [11,16]. MLV Env TM (p15E) is cleaved into p12E and the C-terminal 16-amino-acid long R-peptide at the time of virus budding or shortly thereafter [17]. The R-deleted ecotropic MLV Env induces syncytia in NIH 3T3 cells whereas the wild-type Env does not [18,19].

Previous in vitro studies have shown incomplete inhibition of ecotropic MLV entry in Fv-4 Env-expressing cells [5,6]. This leakage of receptor interference may result in infectious MLV production from the ecotropic MLV-infected cells expressing Fv-4 Env. In the present study, we have examined the effect of Fv-4 Env expression on infectious MLV production from MLV producer cells. Our results showed inhibition of infectious MLV production by Fv-4 Env interacting with the wild-type MLV Env, suggesting contribution of this dominant negative effect to the resistance against ecotropic MLV infection in *Fv-4*-expressing mice.

2. Materials and methods

2.1. DNAs

An ecotropic MLV *env* gene fragment (GenBank accession number X02794 [20]) encoding the wild-type FMLV Env, FE, and an amphotropic MLV *env* gene fragment (GenBank accession number M33469 [21]) encoding the wild-type 4070A Env, AE, were introduced into an expression plasmid, pCXN2 [22], to obtain pCXN2FE and pCXN2AE, respectively. A mutant FMLV Env, FE.D86K [23] (Fig. 1), in which the 86th aspartic acid in FMLV receptor-binding domain was replaced by lysine is equivalent to a previously-reported binding-deficient MoMLV Env mutant, D84K [24]. Like the previously-reported postbinding fusion-defective MoMLV Env whose 461st tyrosine is substituted to proline [25], the 470th tyrosine in FMLV Env and the 455th tyrosine in 4070A Env, equivalent to the 461st tyrosine in MoMLV Env, were replaced by histidine and proline to obtain Env mutants, FE.T470H [23] and AE.T455P, respectively (Fig. 1). The cDNAs encoding the R-deleted FE, R(−)FE, and the R-deleted AE, R(−)AE, were obtained by inserting TAG-stop codon next to the 625th leucine codon in FE and the 610th leucine codon in AE, respectively [23]. An FMLV *env* and a 4070A *env* gene fragments without the stop codon were tagged in frame with an *lck* gene fragment encoding an N-terminal portion (amino acids 5 to 141) of Lck to obtain the Lck-tagged FE, FEL, and the Lck-tagged AE, AEL, respectively, as described previously [26,27]. The cDNAs encoding these Envs were introduced into pCXN2 to obtain pCXN2FE. D86K, pCXN2FE.T470H, pCXN2AE.T455P, pCXN2R(−)FE, pCXN2R(−)AE, pCXN2FEL, and pCXN2AEL, respectively. The *Fv-4* gene [3] was provided by Ikeda, and an *Fv-4 env* gene fragment amplified by PCR was introduced into pCXN2 to obtain pCXN2Fv4E.

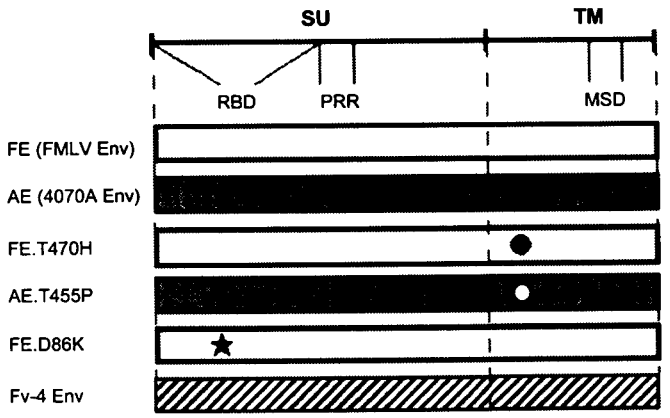

Fig. 1. Structure of MLV Env constructs. FE is the wild-type FMLV Env (indicated by an open box) and AE is the wild-type amphotropic MLV (4070A) Env (indicated by a closed box). FE.T470H is a defective FMLV Env with a point mutation (indicated by a closed circle) in the extracellular domain of TM. AE.T455P is a defective amphotropic MLV Env with a point mutation (indicated by an open circle) in the extracellular domain of TM. FE.D86K is a defective FMLV Env with a point mutation (indicated by a star) in the receptor-binding domain (RBD). Fv-4 Env is indicated by a striped box. PRR represents the proline-rich region in SU and MSD represents the membrane-spanning domain in TM.

2.2. Western blot analysis

Cells were cultured in Dulbecco's modified minimal essential medium supplemented with 10% fetal bovine serum. An MoMLV *gag–pol* producer cell line harboring a lacZ-expressing retroviral vector (MFGnlslacZ), TELCeB6 [28], was provided by Cosset and Takeuchi. For harvesting cellular proteins, cells were plated at a density of 2×10^5 cells per well in 6-well plates, incubated overnight, transfected with 2 μg or indicated amounts of DNAs using Lipofectamine (Invitrogen, Tokyo, Japan), and two days later, were lysed with 0.6 ml of triple-detergent lysis buffer (50 mM Tris-HCl, pH 8.0, 150 mM NaCl, 0.02% sodium azide, 0.1% sodium dodecyl sulfate, 0.5% sodium deoxycholate, 0.1 mg/ml phenylmethylsulfonyl fluoride [PMSF], 1% Triton X-100). For preparing virion proteins, TELCeB6 cells plated at a density of 6×10^5 cells per T25-flask were transfected with 6 μg or indicated amounts of DNAs, and culture supernatants were harvested two days after DNA transfection, filtered through a 0.45-μm-pore-size filter, and centrifuged at 20,600 × *g* for 8 h. The viral pellets from 1 ml of supernatant were lysed with 25 μl of triple-detergent lysis buffer. Each lane was loaded with 10 μl of lysate and Western blot analysis using a polyclonal goat anti-gp70 (MLV SU) antibody (National Cancer Institute, lot 79S000713) was performed as described previously [29].

2.3. Immunoprecipitation analysis

Two days after DNA transfection, cells in a well of 6-well plates were labeled with [35S]redivue Pro-mix (GE Healthcare, Tokyo, Japan) including [35S]methionine and [35S]cysteine for 30 min and were lysed with 0.6 ml of single-detergent lysis buffer (50 mM Tris-HCl, pH 8.0, 150 mM NaCl, 0.02% sodium azide, 0.1 mg/ml PMSF, 1% Triton X-100).

Immunoprecipitation analysis using the anti-gp70 or a polyclonal rabbit anti-Lck antibody (Millipore, Tokyo, Japan) was performed as described previously [27].

2.4. Measurement of viral infectious titers

TELCeB6 cells plated at a density of 2×10^5 cells per well in 6-well plates were transfected with DNAs and two days later culture supernatants were harvested, filtered through a 0.45-μm-pore-size filter, and frozen until use. For measurement of viral infectious titers of these supernatants on NIH 3T3 cells, cells were seeded in 24-well plates (4×10^4 cells per well) and grown overnight. Infections were carried out by plating 0.5 ml of serially diluted viral supernatants in duplicate on NIH 3T3 cells in the presence of polybrene (8 μg/ml; Sigma–Aldrich, Tokyo, Japan), and after 4 h incubation, the virus-containing medium was replaced with fresh medium. Two days later, X-Gal (5-bromo-4-chloro-3-indolyl-b-D-galactopyranoside) staining was performed and the numbers of LacZ-positive colonies were counted to determine end-point viral titers. A representative result of two sets of experiments is shown in each figure.

2.5. Syncytia assay on NIH 3T3 cells

NIH 3T3 cells were plated at a density of 8×10^4 cells per well in 24-well plates, incubated overnight, and transfected with DNAs. One day later, numbers of syncytia were counted.

3. Results

3.1. Fv-4 Env expression

In the present study, we used plasmids expressing the wild-type FMLV Env (FE), the wild-type amphotropic MLV Env (AE), a defective FMLV Env with a mutation in the receptor-binding domain of SU (FE.D86K), a defective FMLV Env with a mutation in the extracellular domain of TM (FE.T470H), a defective amphotropic MLV Env with a mutation in the extracellular domain of TM (AE.T455P), and Fv-4 Env, respectively (Fig. 1). These Env-expression plasmids were transfected into TELCeB6 cells, MoMLV *gag–pol* producer cells harboring MFGnlslacZ retroviral vector. Western blot analysis of cell lysates using an anti-MLV SU (anti-gp70) confirmed expression and processing of these Envs including Fv-4 Env (Fig. 2A). In

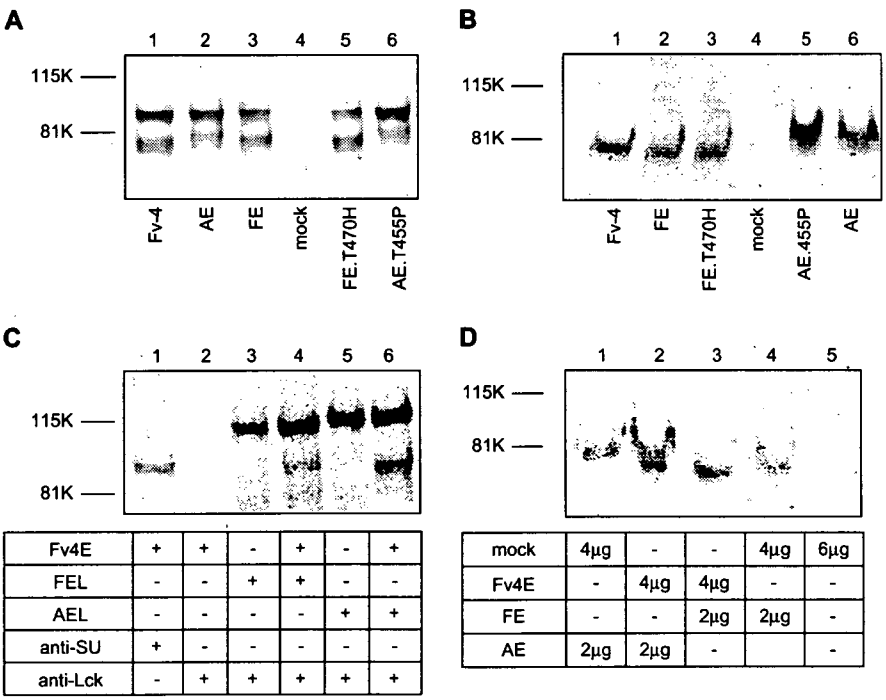

Fv4E	+	+	-	+	-	+
FEL	-	-	+	+	-	-
AEL	-	-	-	-	+	+
anti-SU	+	-	-	-	-	-
anti-Lck	-	+	+	+	+	+

mock	4μg	-	-	4μg	6μg
Fv4E	-	4μg	4μg	-	-
FE	-	-	2μg	2μg	-
AE	2μg	2μg	-		-

Fig. 2. Protein analyses. (A) Western blot analysis of cellular proteins. Lysates of TELCeB6 cells transfected with pCXN2Fv4E (lane 1), pCXN2AE (lane 2), pCXN2FE (lane 3), pCXN2 (mock) (lane 4), pCXN2FE.T470H (lane 5), and pCXN2AE.T455P (lane 6) were subjected to Western blotting using anti-gp70 antibody. (B) Western blot analysis of viral proteins. Lysates of viral pellets prepared from TELCeB6 cells transfected with pCXN2Fv4E (lane 1), pCXN2FE (lane 2), pCXN2FE.T470H (lane 3), pCXN2 (mock) (lane 4), pCXN2AE.T455P (lane 5), and pCXN2AE (lane 6) were subjected to Western blotting using anti-gp70 antibody. (C) Immunoprecipitation analysis. COS cells in a well of 6-well plates were transfected with 1 μg of pCXN2Fv4E (lanes 1 and 2), 1 μg of pCXN2FEL (lane 3), 1 μg of pCXN2FEL plus 1 μg of pCXN2Fv4E (lane 4), 1 μg of pCXN2AEL (lane 5), and 1 μg of pCXN2AEL plus 1 μg of pCXN2Fv4E (lane 6), respectively. Lysates of the labeled cells were subjected to immunoprecipitation analysis using anti-gp70 antibody (lane 1) or anti-Lck antibody (lanes 2–6). Cells were labeled for 30 min and only unprocessed Envs were detected. (D) Western blot analysis of coexpressed viral proteins. TELCeB6 cells in T25-flask were cotransfected with 2 μg of pCXN2AE plus 4 μg of pCXN2 (lane 1), 2 μg of pCXN2AE plus 4 μg of pCXN2Fv4 E (lane 2), 2 μg of pCXN2FE plus 4 μg of pCXN2Fv4 E (lane 3), 2 μg of pCXN2FE plus 4 μg of pCXN2 (lane 4), 6 μg of pCXN2 (lane 5), respectively, as shown in the lower panel. Lysates of viral pellets prepared from the supernatants were subjected to Western blotting using the anti-gp70 antibody.

the electrophoresis, the mobility of the processed Fv-4 Env, Fv-4-SU, was similar with that of FMLV Env SU, and slightly faster than that of amphotropic MLV Env SU. Western blot analysis of viral proteins obtained from supernatants of these transfected cells confirmed that all the Envs including Fv-4 Env were incorporated into the virion (Fig. 2B).

To examine interaction between Fv-4 and the wild-type MLV Envs, immunoprecipitation analysis using Lck-tagged FE and AE (FEL and AEL) was performed (Fig. 2C). FEL or AEL expression was not inhibited by Fv-4 Env coexpression. Fv-4 Env was coimmunoprecipitated with Lck-tagged FE by a monoclonal anti-Lck antibody. It was also coimmunoprecipitated with Lck-tagged AE by this antibody. These results indicate interaction of Fv-4 Env with amphotropic MLV Env as well as FMLV Env.

Then, we examined incorporation of coexpressed wild-type and Fv-4 Envs into the virion. In Fig. 2D, the amount of the incorporated SU detected in lane 3, the sum of FE-SU and Fv-4-SU, looked larger than that of the incorporated FE-SU detected in lane 4. Similarly, the sum amount of AE-SU and Fv-4-SU in lane 2 looked larger than the AE-SU amount in lane 1.

3.2. Inhibitory effect of Fv-4 Env on infectious MLV production

TELCeB6 cells expressing wild-type MLV Envs produce infectious pseudotyped MLVs bearing the Envs. We then examined the effect of Fv-4 Env coexpression on infectious pseudotyped MLV production from these cells. TELCeB6 cells were cotransfected with pCXN2FE and other expression plasmids at 1:2 molar ratio of the former to the latter, and infectious MLV titers in the supernatants were examined (Fig. 3A). While supernatant from TELCeB6 cells expressing FE.D86K, FE.T470H, AE.T455P, or Fv-4 Env alone did not show infectivity on NIH 3T3 cells (data not shown), the control supernatant from TELCeB6 cells transfected with pCXN2FE (plus mock plasmid) showed a titer of more than 1×10^4 IU (infectious units)/ml. Cotransfection of pCXN2FE.D86K had little effect on the titer, but pCXN2FE.T470H cotransfection resulted in approximately 10-fold decrease in the titer. Inhibitory effect of pCXN2Fv4E-cotransfection was more profound, and the titer of the supernatant from TELCeB6 coexpressing FE and Fv-4 Env was less than 1/100 of the control.

Next, we examined the effect of Fv-4 Env that can interact with AE as well as FE on infectious amphotropic MLV production by measuring infectious MLV titers in supernatants from TELCeB6 cells coexpressing AE and other Envs (Fig. 3B). The control supernatant from TELCeB6 cells transfected with pCXN2AE (plus mock plasmid) showed a titer of more than 1×10^4 IU/ml on NIH 3T3 cells. In contrast, the supernatant from TELCeB6 cells cotransfected with pCXN2AE plus pCXN2Fv4E showed much lower infectious titer, less than 1/50 of the control. These results indicate inhibitory effect of Fv-4 Env on infectious ecotropic and amphotropic MLV production.

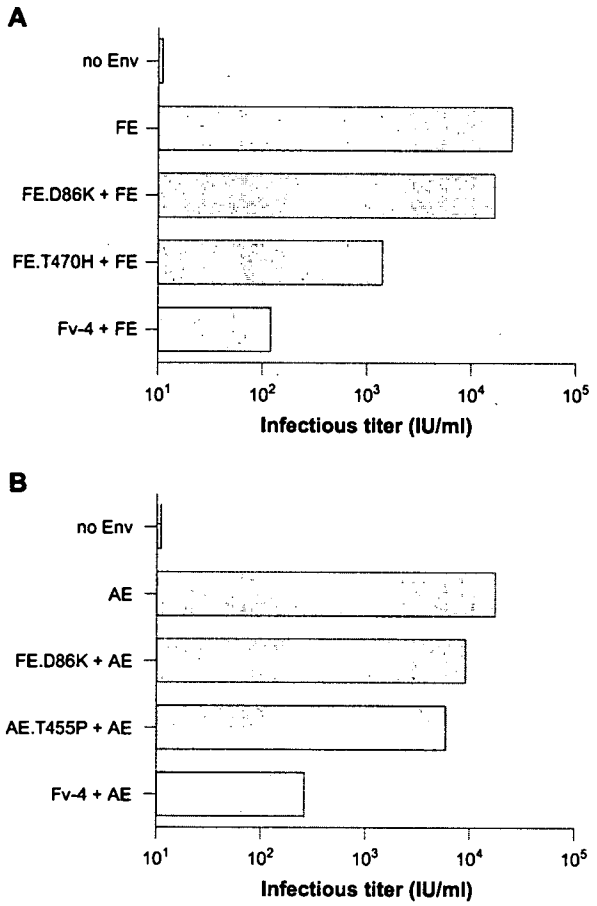

Fig. 3. Infectious viral titers on NIH 3T3 cells of supernatants from TELCeB6 cells coexpressing wild-type and mutant/Fv-4 Envs. (A) TELCeB6 cells were transfected with pCXN2 (no Env) or pCXN2FE (FE) or cotransfected with pCXN2FE and pCXN2FE.D86K (FE.D86K + FE), pCXN2FE.T470H (FE.T470H + FE), or pCXN2Fv4 (Fv-4 + FE) at 1:2 molar ratio of pCXN2FE to mutant/Fv-4 Env-expression plasmid. (B) TELCeB6 cells were transfected with pCXN2 (no Env) or pCXN2AE (AE) or cotransfected with pCXN2AE and pCXN2FE.D86K (FE.D86K + AE), pCXN2AE.T455P (AE.T455P + AE), or pCXN2Fv4 (Fv-4 + AE) at 1:2 molar ratio of pCXN2AE to mutant/Fv-4 Env-expression plasmid. Infectious titers of supernatants from these cells are shown.

We confirmed this inhibitory effect by cotransfection at different molar ratios of pCXN2FE or pCXN2AE to pCXN2Fv4E (Fig. 4). Lower ratio resulted in lower infectious MLV titer in supernatant. Remarkably, cotransfection with pCXN2FE and pCXN2Fv4E at the ratio of 1:3 resulted in decrease in the titer to be undetectable.

3.3. Inhibitory effect of Fv-4 Env on syncytia formation

Syncytia are not induced by wild-type MLV Env but by R-deleted Env in NIH 3T3 cells [18,19]. We then examined the effect of Fv-4 Env coexpression on syncytia formation by R-deleted FE (Fig. 5A). In NIH 3T3 cells, coexpression of FE with R-deleted FE induced larger number of syncytia than those by the R-deleted FE alone, whereas coexpression of FE.T470H resulted in decrease in the number. Fv-4 Env coexpression showed larger inhibitory effect on syncytia formation by R-deleted FE.

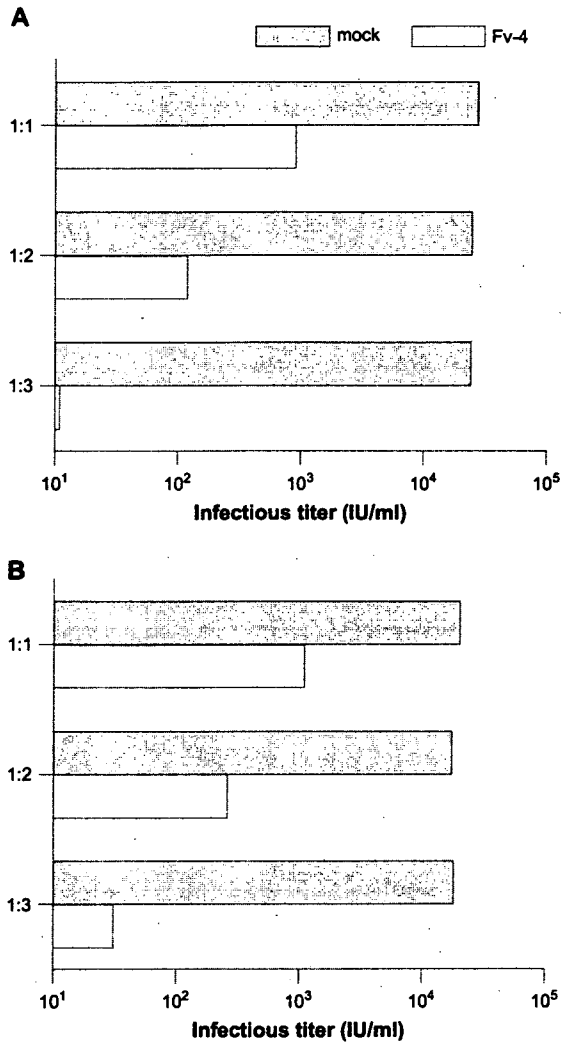

Fig. 4. Infectious viral titers on NIH 3T3 cells of supernatants from TELCeB6 cells coexpressing wild-type and Fv-4 Envs at different molar ratios. TELCeB6 cells were cotransfected with pCXN2FE (A) or pCXN2AE (B) and pCXN2 (mock) or pCXN2Fv4E (Fv-4) at different molar ratios (1:1, 1:2, and 1:3). Infectious titers of supernatants from these cells are shown.

We also examined the effect of Fv-4 Env coexpression on syncytia formation by R-deleted AE (Fig. 5B). Coexpression of AE with R-deleted AE resulted in decrease in syncytia number, and syncytia formation was impaired largely by coexpression of AE.T455P. Coexpression of FE induced larger number of syncytia while FE.T470H coexpression induced similar number compared with the control induced by R-deleted AE alone. Syncytia number induced by coexpression with Fv-4 Env and R-deleted AE was less than one-third of the control. Thus, Fv-4 Env coexpression impaired syncytia formation induced by R-deleted amphotropic as well as ecotropic MLV Envs.

4. Discussion

In the present study, Fv-4 Env coexpression resulted in reduction of infectious MLV titer in supernatant from TELCeB6 cells expressing the wild-type FMLV Env, indicating inhibitory effect of Fv-4 Env on infectious FMLV production from FMLV-infected cells. This may contribute to efficient resistance against ecotropic MLV infection in *Fv-4*-expressing mice. Interestingly, our results also indicate inhibitory effect of Fv-4 Env on infectious amphotropic MLV production, while this effect on amphotropic MLV replication may be limited [6].

Fv-4 Env was shown to be processed and incorporated into MLV virion as reported previously [30], and was indicated to interact with the wild-type Env to form hetero-oligomers. Thus, it can be speculated that TELCeB6 cells cotransfected with pCXN2FE and pCXN2Fv4E expressed FE homo-oligomers, Fv-4 Env homo-oligomers, and FE-Fv-4 Env hetero-oligomers and produced pseudotyped MLVs bearing these oligomers. FE homo-oligomers are functional, whereas Fv-4 Env oligomers are defective and unable to mediate viral entry. Large reduction in infectious titer of MLVs bearing FE and Fv-4 Env (Fig. 3A) suggests reduction in functional Env oligomers on the virion, implying that FE-Fv-4 Env hetero-oligomers are non-functional or unable to mediate viral entry efficiently. Our result in Fig. 2D indicates that TELCeB6 cells cotransfected with pCXN2FE and pCXN2Fv4E produced MLVs bearing both FE and Fv-4 Env, but this does not exclude a possibility of partial reduction in incorporation efficiency of FE-Fv-4 Env hetero-oligomers that may contribute to reduction in infectious MLV titer. Suppression of R(−)FE-mediated syncytia formation by Fv-4 Env coexpression suggests impairment of fusion function of these hetero-oligomers. Thus, Fv-4 Env can exert dominant negative effect on wild-type MLV function. The postbinding defective FE.T470H also suppressed infectious MLV production, but Fv-4 Env showed more profound inhibitory effect. This implies possible contribution of multiple determinants in Fv-4 *env* to this dominant negative effect, consistent with a previous report indicating contribution of Fv-4 SU as well as Fv-4 TM to the defect in Fv-4 Env function [10,30].

Binding of the defective Fv-4 Env to the ecotropic MLV receptor may contribute to the reduction in infectious titer of pseudotyped MLVs bearing FE and Fv-4 Env by interfering with FE binding to the receptor. Our results, however, revealed inhibitory effect of Fv-4 Env on infectious amphotropic MLV production and syncytia formation by R-deleted amphotropic MLV Env, confirming dominant negative effect of Fv-4 Env on wild-type MLV Env function.

In syncytia assay (Fig. 5), FE-coexpression with R(−)FE increased syncytia levels as compared with the mock control, reflecting larger numbers of fusion-competent oligomers (R[−]FE homo-oligomers and FE-R[−]FE hetero-oligomers) in the former. On the contrary, AE-coexpression with R(−)AE decreased syncytia levels as compared with the mock control. The discrepancy may be due to less fusion-activity of AE-R(−)AE hetero-oligomers.

Mice carrying the *Fv-4* gene show extremely efficient resistance to Friend virus infection [2,5]. While involvement of immune responses in the resistance have been indicated [8,9], the receptor interference by Fv-4 Env has been indicated to play a central role in the *Fv-4*-mediated resistance. However, the

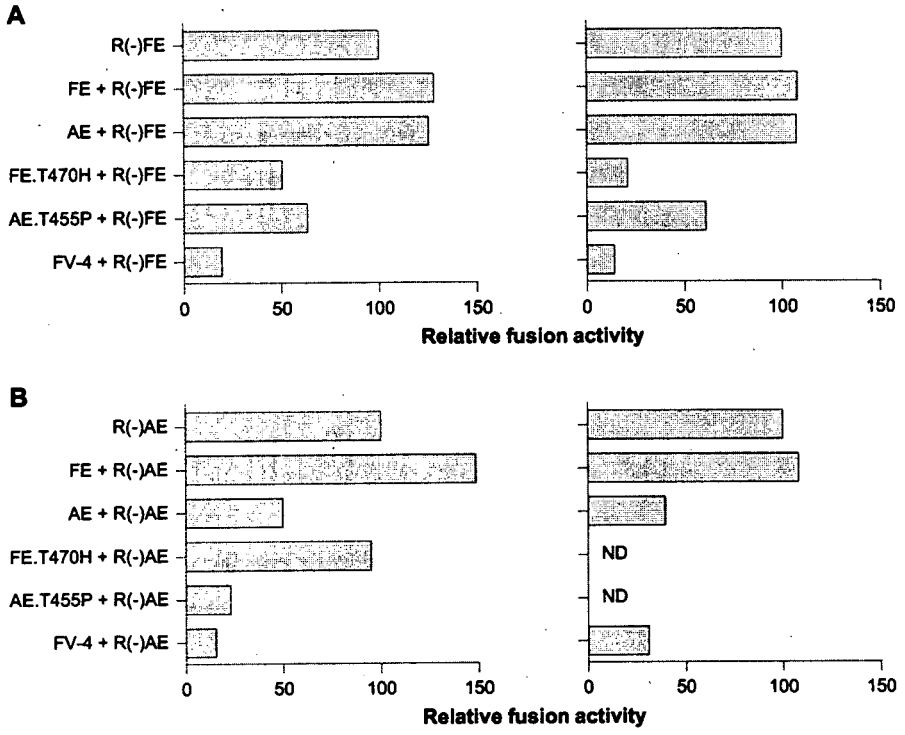

Fig. 5. Syncytia assay on NIH 3T3 cells. NIH 3T3 cells in a well of 24-well plates were cotransfected with 0.02 μg of pCXN2R(−)FE plus 0.04 μg of DNAs expressing the indicated Envs (A) or with 0.1 μg of pCXN2R(−)AE plus 0.2 μg of DNAs expressing the indicated Envs (B), respectively. Syncytia level is shown as a relative value compared to that obtained by mock-cotransfection (R[−]FE in [A] and R[−]AE in [B]) which is rated as 100. Two sets of experiments are shown. ND, not determined.

Fv-4 Env-mediated receptor interference does not result in complete block of FMLV entry into the cells in vitro [5,6]. The mechanism indicated in the present study, Fv-4 Env-mediated interference with the wild-type Env function would reinforce the resistance against Friend virus infection in mice carrying the *Fv-4* gene.

Acknowledgments

This work was supported by a grant from the Ministry of Education, Culture, Sports, Science, and Technology, and a grant from the Ministry of Health, Labor, and Welfare in Japan.

We thank J. Miyazaki for giving us pCXN2 DNA, H. Ikeda for giving us *Fv-4* gene, R. M. Perlmutter and T. Taniguchi for giving us a cDNA encoding Lck kinase, F.-L. Cosset and Y. Takeuchi for giving us TELCeB6 cells, and H. Nakamura and H. Yoshikura for their help.

References

[1] S. Suzuki, *Fv-4*; a new gene affecting the splenomegaly induction by Friend leukemia virus, Jpn. J. Exp. Med. 45 (1975) 473–478.

[2] H. Ikeda, T. Odaka, Cellular expression of murine leukemia virus gp70-related antigen on thymocytes of uninfected mice correlates with *Fv-4* gene-controlled resistance to Friend leukemia virus infection, Virology 128 (1983) 127–139.

[3] H. Ikeda, F. Laigret, M.A. Martin, R. Repaske, Characterization of a molecularly cloned retroviral sequence associated with *Fv-4* resistance, J. Virol. 55 (1985) 768–777.

[4] H. Ikeda, K. Kato, T. Suzuki, H. Kitani, Y. Matsubara, S. Takase-Yoden, R. Watanabe, M. Kitagawa, S. Aizawa, Properties of the naturally occurring soluble surface glycoprotein of ecotropic murine leukemia virus: binding specificity and possible conformational change after binding to receptor, J. Virol. 74 (2000) 1815–1826.

[5] H. Yoshikura, T. Odaka, Resistance of G mice to murine leukemia virus infection: apparent disparity in in vivo and in vitro resistances, J. Natl. Cancer Inst. 61 (1978) 461–463.

[6] H. Yoshikura, Y. Naito, K. Moriwaki, Unstable resistance of G mouse fibroblasts to ecotropic murine leukemia virus infection, J. Virol. 29 (1979) 1078–1086.

[7] M. Kitagawa, S. Aizawa, H. Kamisaku, H. Ikeda, K. Hirokawa, T. Sado, Cell-free transmission of *Fv-4* resistance gene product controlling Friend leukemia virus-induced leukemogenesis: a unique mechanism for interference with viral infection, Blood 86 (1995) 1557–1563.

[8] K. Higo, Y. Kubo, Y. Iwatani, T. Ono, M. Maeda, H. Hirai, T. Masuda, K. Kuribayashi, F. Zhang, T.Y. Lamin, A. Adachi, A. Ishimoto, Susceptibility of nude mice carrying the *Fv-4* gene to Friend murine leukemia virus infection, J. Virol. 71 (1997) 750–754.

[9] F. Zhang, L.T. Ya, Y. Iwatani, K. Higo, Y. Suzuki, M. Tanaka, T. Nakahara, T. Ono, H. Sakai, K. Kuribayashi, A. Ishimoto, Resistance to Friend murine leukemia virus infection conferred by the *Fv-4* gene is recessive but appears dominant from the effect of the immune system, J. Virol. 74 (2000) 6193–6197.

[10] G.M. Taylor, Y. Gao, D.A. Sanders, *Fv-4*: identification of the defect in Env and the mechanism of resistance to ecotropic murine leukemia virus, J. Virol. 75 (2001) 11244–11248.

[11] E. Hunter, Viral entry and receptors, in: J.M. Coffin, S.H. Hughes, H.E. Varmus (Eds.), Retroviruses, Cold Spring Harbor Laboratory Press, New York, 1997, pp. 71–120.